UNIVERSITY OF READING

Department of Mathematics

Slow and superfast diffusion of contaminant species through porous media

Amanda Hynes

A dissertation submitted in partial fulfilment of the requirement for the degree of

Master of Science, Mathematics of Scientific and Industrial Computation

August 2014

Acknowledgements

I would like to thank my supervisor Prof. Mike Baines, for his help, encouragement and advice throughout this project. Additionally I would like to thank my maths mentor at AWE, Dr. Pete Spence, for his help, encouragement and support throughout the MSc. Thanks are also due to Dr. Alex Lukyanov for helpful conversations and I would finally I would like to thank AWE for financial support.

Declaration

I confirm that this is my own work, and the use of all material from other sources has been properly and fully acknowledged.

Signed.. Date...................

Abstract

This dissertation describes a finite difference moving mesh method to model the diffusion of a homogenous non reacting solvent through a porous material based on two regions, for slow and superfast diffusion. These regions are joined at an interface position. The slow and superfast regimes are governed by different forms of the nonlinear porous medium equation. The numerical method, which is based on conservation, is derived in detail and discussed. Velocities are calculated for spatial nodes on a 2-dimensional radial mesh, and as a result the position and solution at the spatial nodes are updated at each time step as the solvent spreads. The calculation of velocities requires knowledge of the masses between adjacent nodes, which change with time. The results of the numerical model are presented, the limitations of the success of the model being dependent on temporal step sizes. Such moving mesh methods are useful in helping to model the transport of contaminant species through soil/sand systems, thus enabling the prediction of the fate of such contaminants in the environment.

Contents

List of Figures

1   Introduction

The migration of contaminants or reactants through porous media is of critical importance for a wide variety of scientific and industrial processes. This process can include both reaction with and without the porous media. [1] Contamination of soils and sands for example, by liquid pollutants can result in those pollutants entering groundwater systems, thus increasing the chance of harm to crops and ecosystems, and water supplies to the public. It is important therefore to characterise such phenomena, and be able to predict the fate of such species, dependent on porous media and pollutant type, over a wide range of conditions. It is known that the nonlinear diffusion of unreactive pollutants can be classified into *slow*, *fast* or *superfast* diffusion, dependent on the characteristics of the diffusion coefficient in the porous medium equation. The diffusion coefficient is often dependent on the saturation level of the contaminant species in the porous medium, which drives the diffusion. This changes over time as the solution spreads out through the voids.

This project looks at the concentration profile of a contaminant species of a particular initial concentration through a porous medium (of which there are many in the environment, such as sands and soils) with time. The diffusion equation is of the nonlinear type, and the type of diffusion changes at a particular distance away from the initial point of contact with the solid, from slow to fast, to superfast diffusion, as the saturation level / concentration of the species changes. We model this using a finite difference moving mesh, by assigning a velocity to each positional node in matrix, which changes with time, and then advancing those nodal positions and calculating the new positions and concentrations at evenly spaced time steps. As mass is not conserved within the separate slow and superfast regimes, we use mass fraction conservation between positional nodes. The combined sum of the masses in both the slow and fast sections remain constant.

---

[1]A porous medium is a solid matrix, or framework containing pore / voids. They are often characterised mainly by their porosity, or void fraction, which is the fraction of empty space within the solid matrix.

1.1 Background to diffusion through porous media

Migration of non reacting liquids through porous media is driven by the capillary forces at the liquid front. The liquid passes through voids between the solid particles within the packed solid matrix. The liquid will travel through large gaps between the particles, and narrow gaps where the particles are in near contact. At low liquid concentrations, as the liquid spreads out through the matrix, the capillary structure breaks down, and the liquid passes over the rough surfaces of the particles. The thin layer of liquid between particles are referred to as capillary bridges, as shown in Figure 1.
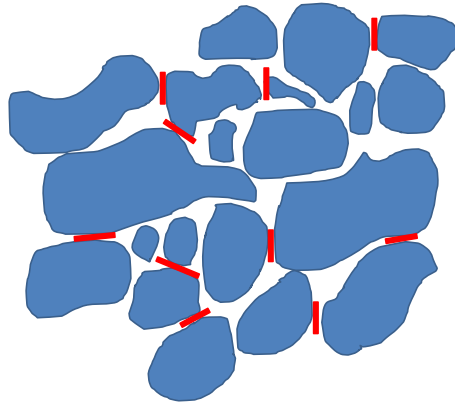
Figure 1: Porous medium structure, illustrating varying particle shape and size, and location of thin capillary bridges (red bars) between particles. Thin layer of liquid on surface roughness or particles where not in contact, at low concentration (not shown).

The rough surfaces can be well characterised by techniques such as scanning electron microscopy (SEM), atomic force microscopy (AFM) for nanoscale measurements, and surface profilometry, of the stylus or optical type. The free space percentage, or void fraction can be determined by a variety of methods, such as optical techniques, imbibition methods (full wetting of the voids), mercury injection methods, gas expansion methods and density methods. More details on these methods, and other characterisation requirements such as permeability, and specific surface area can be found in [1]. The classification of nonlinear diffusion can be subdivided into *slow*, *fast*, or *superfast* diffusion, dependent of the value of m in the nonlinear diffusion equation, where

$$\frac{\partial u}{\partial t} = \frac{\partial}{\partial x}\left(u^m \frac{\partial u}{\partial x}\right) + s(x),$$

is the porous medium equation (PME) in $1D$ Cartesian coordinates. It can be generally stated as

$$\frac{\partial u}{\partial t} = \frac{\partial}{\partial x}\left(D\left(u(x(t),t)\right)\frac{\partial u}{\partial x}\right) + s(x),$$

where $D(u(x(t),t))$ is the diffusion coefficient (which, when $D(u) = u^m$, is the PME). For radial diffusion, the nonlinear PME is given by

$$\frac{\partial u}{\partial t} = \frac{1}{r^{d-1}}\frac{\partial}{\partial r}\left(u^m r^{d-1}\frac{\partial u}{\partial r}\right) + s(r), \qquad (1)$$

where d is the number of dimensions. In this study we take $d = 2$. For both radial and cartesian coordinates, $s(x(t))$ and $s(r(t))$ represent a *source* or *sink* term, such as ingress of another source of liquid into the system, or evaporation of the liquid out of the system respectively. In the case of this study, we do not consider any source or sink terms, particularly since we assume that our migrating liquid is a non reacting, non volatile liquid.

The transition of transport through porous media is very much dependent on the saturation level of the solvent. This change in diffusion behavior can be very sharp as detailed in the study by Lukyanov *et al* [2]. This transition is seen to occur at about 20% saturation for low saturation levels. The general classification of the "speed" of non linear diffusion with respect to the value of m in equation (1), according to reference [3] is

- **linear:** $m = 0$

- **porous medium equation:** $m > 0$

- **fast diffusion:** $-1 < m < 0$

- **superfast diffusion:** $m < -1$

In this report we look at the profile of concentration $u(r(t),t)$ with time, where the diffusive behaviour changes from slow to superfast diffusion. At this point the concentration (u) in the profile of u against r is 20% of its value at the central point $r = 0$, where the solvent is "applied". This is in agreement with the observations of reference [2]. We firstly calculate the position at which the diffusion regime changes, at time $t(0)$, then follow the profile in time using two joined moving mesh methods

for slow ($m = 1$) and superfast ($m = -3/2$) diffusion. Where the concentration $u(r)$ is greater than 20% of $u(r = 0)$, for $m = 1$, we present a self similar/analytic solution for $u(r(t), t)$, which is used to obtain the boundary values of the velocity ($\mathrm{d}r/\mathrm{d}t$), rate ($\partial u/\partial t$) and gradient ($\partial u/\partial r$) of the positional node at the slow/superfast interface, in order to set up a moving mesh method for the fast regime only. Applying a parabola from this node out to the final node, furthest from the origin (where we can apply a boundary condition to advance capillary action), we can then update the position of the fast nodes using their velocities at equally spaced time steps to advance the mesh. We can then find the solution values u at the new positions, making use of constant mass fractions flowing across the boundary from the slow to superfast regime.

The study in reference [2] has provided an insight into the behaviour of non volatile liquids at low concentrations, and how the liquid flows at such low saturation levels. At low saturation levels, below 20%, Lukyanov *et al* [2] found that the spreading regime changed. The study looked into the effect of low concentrations (less than $5\mu L$) of a nonvolatile organic solvent (non-volatile to ensure that there is no source/sink term for liquid leaving or entering the region) through a well characterised sand [2]. The passage of the volatile solvent through the sand was monitored over time using imaging techniques such as Micro X-ray Computer Tomography, Fluorescence Imaging and Raman Microscopy. The imaging following the profile of the wetting front [3], is shown in Figure 2.

---

[2]of known porosity and surface roughness.
[3]The wetting front is the region in the porous medium with a rapid downward decrease in water content, at the wetted and dry interface.
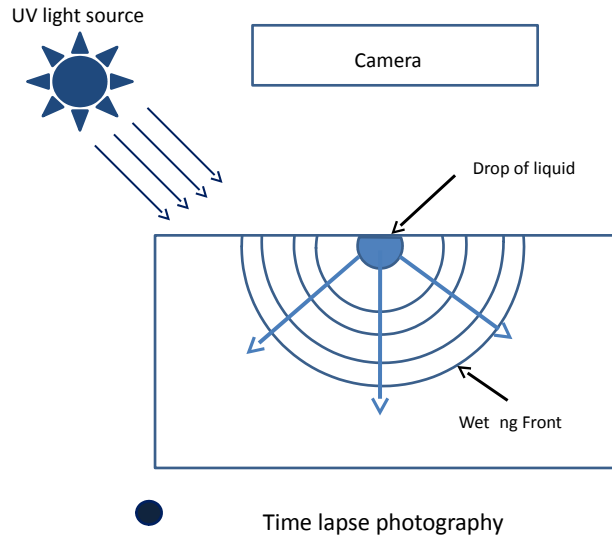
Figure 2: X-Ray Fluorencence Imaging to monitor progress of wetting front

It was seen that for a very small concentration of solvent initially placed on the surface of the sand, the spreading, over a period of 25 days, covered a volume of 1000 times that of the original spreading volume at time $t(0)$ for a porosity/void fraction of 30%[4]. This indicated an average saturation level of approximately 0.55% [5].

Different liquid morphologies are seen around the solid particles at different levels of saturation and at saturation levels of less than 8%, liquid bridges are formed at the point of contact between particles, at which point the larger capillary areas, as shown in Figure 3 collapse. Indeed, below a saturation level of 0.2%, cohesion is lost in the system, and the bridge network fails between particles.

---

[4]Porosity is the fraction of total volume of a material that is free space.
[5]Saturation level $s = \frac{\text{volume of fluid phase } i \text{ in sample}}{\text{Total accessible pore volume in sample}}$.
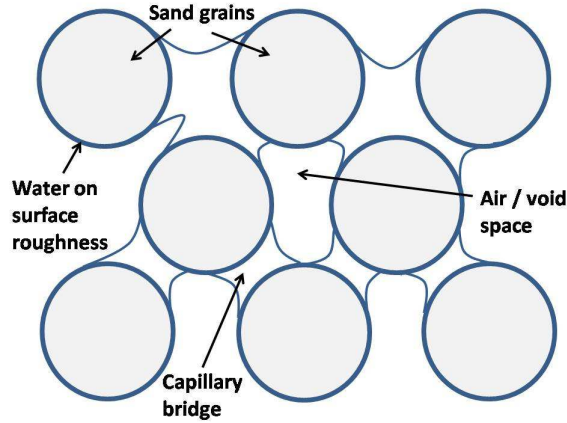
Figure 3: Structure of capillary areas between sand particles at saturation levels greater than 10%

This paper provided evidence, from an environmental pollution perspective, that small concentrations of harmful solvents can travel long distances through packed soils/sands over long periods of time, thus justifying the requirement to investigate the migration of harmful contaminant species.

The transport of liquid through the porous media was deduced to be due to capillary action at the surface-roughness scale of the individual particles, and indeed the total saturation of the sand is the interplay between that within the capillary bridges, and that in the surface roughness around the particles. Generally, the flow obeys a Darcy-like Law, where permeability is related to the geometry of the grooves [4]. In macroscopic modelling of the migration of the nonvolatile liquid, it was assumed that the particles were perfect spheres, and that the wetted grooves within the surface roughness of the particles were completely filled. Modelling results were then compared to those obtained from experiments. A continuity equation was then generated

$$\frac{\partial \phi s}{\partial t} + \nabla \cdot \mathbf{q} = 0,$$

where ϕ is the porosity, s the total saturation, and $\mathbf{q}$ is the flux, which, when combined with Darcy's Law and the gradient of the capillary pressure and liquid geometry calculations for capillary pressure, results in a porous medium equation

$$\frac{\partial s}{\partial t} = \nabla \cdot \left(s^{\gamma - 1} \nabla s \right),$$

following non-dimensionalisation, for saturation, distance and time. When comparing to equation (1), $\gamma = m + 1$. This is known as *superfast diffusion*. In the standard porous medium equation (which we will use for the slow section of our model), where $m > 1$ in equation (3), the low saturation levels at the edge of the liquid delay the onset of the wetting front, however (and in our model for superfast diffusion), for superfast regimes, the velocity of the wetting front decreases over time as the saturation level/concentration decreases. The results of the model are in agreement with experiment, and for the characterised system with the organic solvent, trioctyl-phosphate (TEHP) at low concentration (deposited on well characterised sand) the superfast diffusion regime is said to hold for $0.5\% < s < 10\%$. It was also shown that the wetted volume, V fell on a power law with time, where $V \propto t^{0.75}$ as shown in Figure 4.
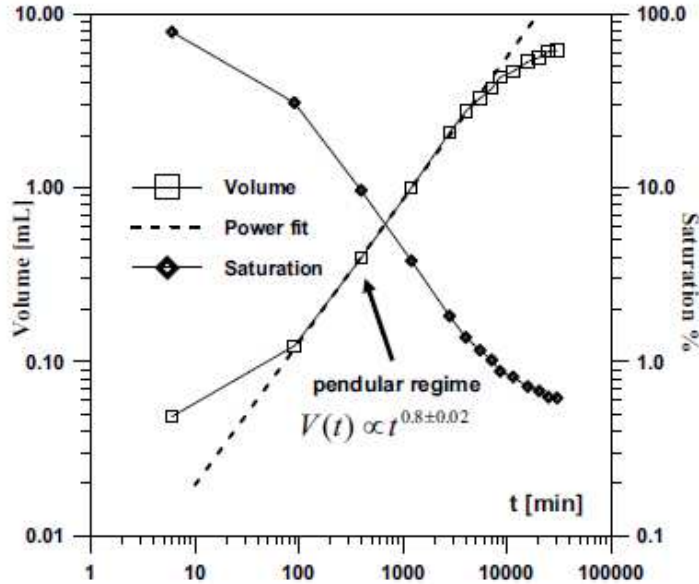
Figure 4: Migration of $11\mu L$ TEHP in well characterised sand, showing $V \propto t^{\approx 0.75}$, from reference [2].

Aside from the migration of contaminants, the moving mesh method has been used for biological problems, such as tumour growth as described in reference [5].

1.2 Velocity based moving mesh method

This project involves the use of velocity based moving numerical mesh methods (specifically in this case, a finite difference method), to investigate the time dependent migration / nonlinear diffusion of a contaminant species. Moving mesh methods have been utilised for scientific applications, such as diffusion of heat, diffusion of contaminant species through porous media (as in this study), and many biological applications, such as migration of species, and advancing of tumours through tissue. They are also known as Lagrangian methods, where the velocity of the nodal points in a discretised domain are calculated for each time step, and these velocities are used to aquire future positions of the nodes, and hence the solution values required at the next time step. This velocity is therefore directly used in the time dependent PDE. Considering the Lagrangian coordinate, $\mathbf{x}(t)$ in $3D$, at time t, the velocity $\mathbf{v}(\mathbf{x}, t)$ of the diffusing species at a node in the dicretised domain is given by

$$\mathbf{v} = \frac{\partial \mathbf{x}}{\partial t},$$

where $\mathbf{x}(t)$ is the position of the node within the discretised mesh at time t (each node moves at velocity $\mathbf{v}(\mathbf{x}, t)$ at time t). One of the main problems with moving meshes is, however, for the mesh to become "'tangled", where nodes start to overtake one another, and this should be considered in the assignment of spatial and temporal discretisation. A more in depth discussion into moving meshes, with theory, to solve time dependent partial differential equations can be found in reference [6].

1.3 Overview of the project

The aim of this project has been to develop a moving mesh method for combined slow and superfast diffusion, which is intuitive since at initial time, the concentration profile (concentration u, or saturation s, as a function of distance from the central point of application of the solvent) will, as distance increases from the central point, decrease to a level of approximately less than 30% of the central concentration. At this point, m decreases in the porous medium equation, and the diffusion regime will move from slow, to fast $m < 0$, to superfast, $m < -1$ (where $u \leq 8\%$). This project aims to "join" the two regimes at an interface nodal position, and we choose this to

occur where the solution value for concentration (or saturation) is 20% of its maximum value. As expected, the central node will not move, however, the other nodes in the mesh will move with a velocity that changes with time. This is a first attempt at finding a method to combine the regimes, requiring careful consideration of boundary conditions, both at the central node, interface node, and final node, furthest from the origin. A finite value is assigned to the solution at the farthest node from the origin.

We have already introduced the concept in this first chapter as to the rationale behind studying the migration of contaminants through porous media, and why it is important to develop predictive models to understand the fate of these contaminants, and the different classifications of nonlinear diffusion dependent on saturation level of the contaminant, (hence value of m). In Chapter 2 we consider slow diffusion, and present a self similar solution for the porous medium equation via scale invariance. It is this self similar solution with which we obtain our boundary values at the interface between slow and superfast diffusion. We also use these interface boundary conditions where we consider superfast diffusion only, with a flux entering the superfast regime. By boundary values, we mean not just the position and solution at the boundary, but the velocity of the interface node for all time.

In Chapter 3 we present methods and proposed algorithms for

1. A moving mesh method for slow diffusion in isolation, driven by conservation of mass between nodes.

2. A moving mesh method for superfast diffusion in isolation, driven by the concept of constant mass fractions between nodes, as mass is no longer constant, effectively entering from the interface side (with what would be slow diffusion if we were considering both regimes). We use the continuity of mass fractions in the regime to update the total mass between nodes, making use of our knowledge of the original mass between nodes at the initial time.

3. A moving mesh method for slow diffusion using mass fraction conservation, in preparation for joining to the superfast diffusion regime.

4. A combined slow and superfast diffusion moving mesh, with use of constant mass fractions.

In Chapter 4 we present the results of the moving mesh methods for both slow and superfast diffusion in isolation for $2D$ radial diffusion, followed by the results for the combined numerical method. In the case of the slow diffusion we show the results for constant mass between spatial nodes. We discuss the stability and limitations on the discretisation of time via a Lagrangian type Courant-Friedrichs-Lewy (CFL) condition [7]. This condition prevents the spatial nodes from overtaking one another.

In Chapter 5 we draw some conclusions from the results, comparing the behaviour of the slow and superfast regimes in isolation with the combined diffusion moving mesh scheme.

In Chapter 6 we make recommendations for future study, drawing on complications and limitations of schemes as a result of explicit finite difference methods.

2   Generation of an analytic solution for slow diffusion

In this chapter we look for an analytic solution to the porous medium equation where $m = 1$, by generating a self similar solution. We shall firstly describe the scale invariance applied to $2D$ radial diffusion, and follow this with the generation of the self similar/analytic solution. This method is discussed in reference [8], and adopted in $1D$ Cartesian coordinates, where $m = 4$, in reference [9].

2.1   Scale invariance for slow diffusion

We consider the case where $m = 1$ and $d = 2$ in the nonlinear porous medium equation (2)

$$\frac{\partial u}{\partial t} = \frac{1}{r^{d-1}}\frac{\partial}{\partial r}\left(r^{d-1}u^m\frac{\partial u}{\partial r}\right) \tag{2}$$

where d is the number of dimensions. We now apply a scaling transformation to equation (2),

$$u = \lambda^\gamma \hat{u}, \quad t = \lambda\hat{t}, \quad r = \lambda^\beta \hat{r}, \tag{3}$$

using the scaling parameter, λ, where α and β are constants. This transforms equation (2) into the new non-dimensionalised variables $\hat{u}$, $\hat{t}$, and $\hat{r}$;

$$\frac{\lambda^\gamma}{\lambda}\frac{\partial \hat{u}}{\partial \hat{t}} = \frac{\lambda^{2\gamma-2\beta}}{\hat{r}^{d-1}}\frac{\partial}{\partial \hat{r}}\left(\hat{u}\hat{r}^{d-1}\frac{\partial \hat{u}}{\partial \hat{r}}\right). \tag{4}$$

Therefore, equating both the left and right hand sides of equation (4),

$$\gamma - 1 = 2\gamma - 2\beta. \tag{5}$$

To find γ and β we need two independent equations, and so we integrate equation (2),

$$\int_0^{b(t)}\frac{\partial u}{\partial t}r^{d-1}\mathrm{d}r = \int_0^{b(t)}\frac{\partial}{\partial r}\left(r^{d-1}u\frac{\partial u}{\partial r}\right)\mathrm{d}r,$$

and apply the boundary condition

$$\frac{\partial u}{\partial r} = 0, \quad \text{at} \quad r = 0,$$

and

$$u(b) = 0 \quad \text{at the boundary} \quad r = b(t).$$

This results in

$$\frac{\partial}{\partial t} \int_0^{b(t)} r^{d-1} u \, \mathrm{d}r = 0,$$

and so

$$\int_0^{b(t)} r^{d-1} u \mathrm{d}r = k, \tag{6}$$

where k is a constant. Upon transformation of equation (6) into $\hat{u}$, $\hat{t}$ and $\hat{r}$ we obtain

$$\lambda^{\beta d} \lambda^\gamma \int_0^{b(t)} \hat{r}^{d-1} \hat{u} \mathrm{d}\hat{r} = \lambda^0 k,$$

thus generating a second equation in γ and β,

$$\gamma + 2\beta = 0. \tag{7}$$

Therefore, solving equations (5) and (7)

$$\beta = \frac{1}{4}, \quad \text{and} \quad \gamma = -\frac{1}{2}.$$

This results in a scale transformation

$$u = \lambda^{-\frac{1}{2}} \hat{u}, \quad t = \lambda \hat{t}, \quad \text{and} \quad r = \lambda^{\frac{1}{4}} \hat{r},$$

so

$$\lambda = \frac{u^{1/\gamma}}{\hat{u}^{1/\gamma}} = \frac{t}{\hat{t}} = \frac{r^{1/\beta}}{\hat{r}^{1/\beta}}.$$

An in depth text on scaling methods and self similarity can be found in reference [11].

2.2 Generation of a self similar solution for slow, nonlinear diffusion

We now introduce two variables, ϕ and y, that are independent of λ, and which are invariant under transformation equation (3). We then make ϕ a function of y, and then transform as follows

$$\phi = \frac{u}{t^\gamma} = \frac{\hat{u}}{\hat{t}^\gamma},$$

$$y = \frac{r}{t^{\beta}} = \frac{\hat{r}}{\hat{t}^{\beta}}.$$

With ϕ now a function of y, we can transform the left hand side of equation (2) to be a function of ϕ and t,

$$
\begin{aligned}
\frac{\partial u}{\partial t} &= \frac{\partial}{\partial t} \left(\phi t^{\gamma} \right) \\
&= -t^{\gamma-1} y \beta \frac{\mathrm{d}\phi}{\mathrm{d}y} + \phi \gamma t^{\gamma-1}.
\end{aligned}
$$

The right hand side of equation (2) is also transformed

$$
\begin{aligned}
\frac{1}{r} \frac{\partial}{\partial r} \left(r u \frac{\partial u}{\partial r} \right) &= \frac{1}{y t^{\beta}} \frac{\partial y}{\partial r} \frac{\mathrm{d}}{\mathrm{d}y} \left(y t^{\beta} \phi t^{\gamma} \frac{\partial y}{\partial r} \frac{\partial u}{\partial \phi} \frac{\mathrm{d}\phi}{\mathrm{d}y} \right), \\
&= \frac{t^{2\gamma - 2\beta}}{y} \frac{\mathrm{d}}{\mathrm{d}y} \left(y \phi \frac{\mathrm{d}\phi}{\mathrm{d}y} \right),
\end{aligned}
$$

where $m = 1$ and $d = 2$, in radial coordinates, to obtain

$$\frac{1}{4} \frac{\mathrm{d}}{\mathrm{d}y} \left(y^2 \phi \right) + \frac{\mathrm{d}}{\mathrm{d}y} \left(y \phi \frac{\mathrm{d}\phi}{\mathrm{d}y} \right) = 0$$

which, following integration gives

$$\frac{1}{4} y^2 \phi + y \phi \frac{\mathrm{d}\phi}{\mathrm{d}y} = C,$$

where C is a constant of integration. If we assume that $\frac{\mathrm{d}\phi}{\mathrm{d}y} = 0$, when $\phi = 0$, then

$$y \left(\frac{1}{4} y \phi \right) + y \phi \frac{\mathrm{d}\phi}{\mathrm{d}y} = 0,$$

hence

$$\frac{y}{4} + \frac{\mathrm{d}\phi}{\mathrm{d}y} = 0.$$

Integrating

$$\int \mathrm{d}\phi = -\frac{1}{4} \int y \mathrm{d}y,$$

$$\phi = -\frac{1}{4} \left(\frac{y^2}{2} + \mathrm{d} \right),$$

13

where d is a constant of integration. Therefore

$$\phi = A - \frac{y^2}{8},$$

where A is a constant. We we can write

$$\phi = A - \frac{y^2}{8}, \quad \frac{y^2}{8} \leq A.$$

$$\phi = \left(A - \frac{y^2}{8}\right)_+.$$

We now convert back to the original variables, $(u(r(t), r(t), t))$;

$$u = \left(\frac{1}{\sqrt{t}}\left(A - \frac{1}{8}\frac{r^2}{\sqrt{t}}\right)\right)_+. \tag{8}$$

Equation (8) is is known as the self-similar solution for 2D non-linear radial diffusion (from a point source of solvent on the surface of a porous medium). This can be applied to nonlinear diffusion cases where $m > 0$.
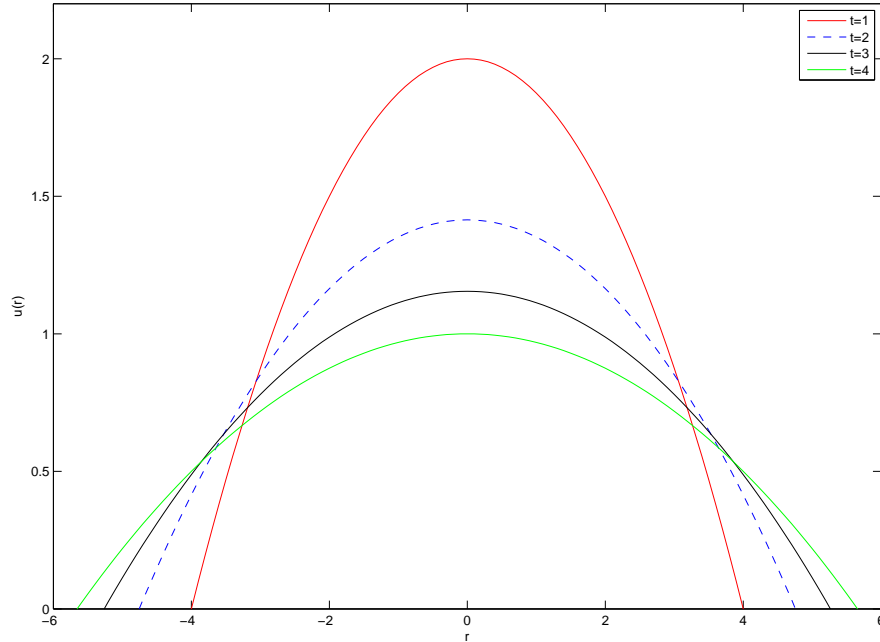
Figure 5: Self similar solution where $m = 1$ at $t = 1, 2, 3$ and 4

14

Figure 5 illustrates the self similar solution, equation (8), where $A = 2$, for the original non-linear $2D$ equation (2), where $d = 2$, $m = 1$. Four time steps are shown. It can be seen that the profile gradually flattens over time and is symmetric about $r = 0$. In this study we take the initial time, $t_0 = 1$ to ensure a stable solution. Additionally, without loss of generality, we assign $A = 2$.

3 A velocity based moving mesh method

In this section we consider the porous medium equation for both slow and superfast diffusion in $2D$ radial coordinates

$$\frac{\partial u}{\partial t} = \frac{1}{r}\frac{\partial}{\partial r}\left(u^m r \frac{\partial u}{\partial r}\right)$$

where $m = 1$ for slow diffusion, and $m = -3/2$ for superfast diffusion. We derive a method to monitor the diffusion of a non volatile species over time, with boundary conditions. We first consider the slow diffusion equation in isolation, in the region $(r_0(t), r_I(t))$, applying boundary conditions

$$\frac{\mathrm{d}r}{\mathrm{d}t} = 0, \quad \frac{\partial u}{\partial r} = 0, \quad \text{at} \quad r_0(t),$$

and

$$u(r_I(t), t) = \frac{1}{5}u(r_0(t), t) \quad \text{at} \quad r_I(t),$$

connecting $r_0(t)$ and $r_I(t)$ with a zero net flux condition at $r_I(t)$ (a free boundary condition)

$$r_I u_I \left.\frac{\partial u}{\partial r}\right|_I + r_I u_I \left.\frac{\mathrm{d}r}{\mathrm{d}t}\right|_I = 0 \quad \text{at} \quad r_I(t),$$

where $\left.\frac{\mathrm{d}r}{\mathrm{d}t}\right|_I$ is the velocity of the boundary at $r_I(t)$. We can show, using Leibnitz Integral Rule that for any two interval points, $r_A(t)$, $r_B(t)$,

$$\frac{\mathrm{d}}{\mathrm{d}t}\int_{r_A(t)}^{r_B(t)} ur\mathrm{d}r = \int_{r_A(t)}^{r_B(t)} r\frac{\partial u}{\partial t}\mathrm{d}r + \left[ur\frac{\mathrm{d}r}{\mathrm{d}t}\right]_{r_A(t)}^{r_B(t)}$$

$$= \int_{r_A(t)}^{r_B(t)} r\left(\frac{1}{r}\frac{\partial}{\partial r}\left(ru\frac{\partial u}{\partial r}\right)\right)\mathrm{d}r + \left[ur\frac{\mathrm{d}r}{\mathrm{d}t}\right]_{r_A(t)}^{r_B(t)}$$

15

$$= \left[ru \frac{\partial u}{\partial r} \right]_{r_A(t)}^{r_B(t))} + \left[ur \frac{\mathrm{d}r}{\mathrm{d}t} \right]_{r_A(t)}^{r_B(t)}$$

$$= \int_{r_A(t)}^{r_B(t)} \left(\frac{\partial}{\partial r} \left(ru \frac{\partial u}{\partial r} \right) + \frac{\partial}{\partial r} \left(ru \frac{\mathrm{d}r}{\mathrm{d}t} \right) \right) \mathrm{d}r \tag{9}$$

Taking $r_A(t) = 0$, $r_B(t) = r_I(t)$, where I denotes the end node (where the interface with the fast diffusion regime would be), we have

$$\frac{\mathrm{d}}{\mathrm{d}t} \int_0^{r_I(t)} ur \, \mathrm{d}r = 0 \tag{10}$$

so the total mass is conserved.

3.1   A moving mesh method for slow diffusion

We define the velocities at points A and B implicitly by

$$\frac{\mathrm{d}}{\mathrm{d}t} \int_{r_A(t)}^{r_B(t)} ur \mathrm{d}r = 0 \tag{11}$$

for any two nodes nodes $r_A(t)$ and $r_B(t)$, which is consistent with equation (10). Then

$$\left. \left(ru \frac{\partial u}{\partial r} + ru \frac{\mathrm{d}r}{\mathrm{d}t} \right) \right|_{r_A(t)}^{r_B(t)} = 0$$

from equation (9), for any points $r_A(t)$ and $r_B(t)$. Take $r_A(t){=}0$, and $r_B(t) = r(t)$, then from equation (9), since $u > 0$

$$\frac{\mathrm{d}r}{\mathrm{d}t} = -\frac{\partial u}{\partial r}, \tag{12}$$

and this is how the grid/mesh points will progress. From equation (11), the integral between any two mesh points, A and B is constant for all time, that is

$$\int_{r_A(t)}^{r_B(t)} ur \, \mathrm{d}r = \text{constant}$$

Now we can advance the mesh in time.

16

Algorithm for slow diffusion alone with mass conservation

Initially:

1. Define the initial condition everywhere to be

$$u(r) = 2 - \frac{r^2}{8} \quad \text{at} \quad t_0 = 1$$

2. Discretise the mesh $r_i(t) = r_0(t) + i\Delta r$, where Δr are N uniform discretisations $i = 0, 1, \ldots, N$, across the domain at t_0.

3. Calculate the initial masses between nodes using Simpson's Rule $b_i = \int_{r_0}^{r_i} ur\,dr$, between the origin at r_0, and nodes i, for $i = 0, \ldots, N$.

Then, at each time step,

1. Calculate the velocities from equation (12), approximating the gradient by suitable finite differences, for example, central differences:

$$\left.\frac{\partial u}{\partial r}\right|_i \approx \frac{u_{i+1}(t) - u_{i-1}(t)}{r_{i+1}(t) - r_{i-1}(t)} \quad i = 1, \ldots, N-1.$$

2. Define the velocity of the final node at r_N through linear extrapolation

$$v_N = 2v_{N-1} - v_{N-2}$$

or by using the one-sided difference

$$v_N \approx -\frac{u_N - u_{N-1}}{r_N - r_{N-1}}.$$

3. Update the new positions at the next time step using the explicit Euler scheme

$$r_i(t + \Delta t) = r_i(t) + \Delta t \left.\frac{dr}{dr}\right|_i,$$

for equally spaced time steps Δt.

4. Update the solutions at the next time step using the new positions from step 3,

$$u_i(t + \Delta t) = \frac{b_{i+1} - b_{i-1}}{r_i(t + \Delta t)\,(r_{i+1}(t + \Delta t) - r_{i-1}(t + \Delta t))}, \quad \text{for} \quad i = 1, \ldots, N-1.$$

5. Calculate u at the origin by approximating the integral/mass between the origin and the first mesh point at $t + \Delta t$,

$$\int_0^{r_1(t+\Delta t)} ur\,\mathrm{d}r \approx \frac{1}{4}\left(u_0(t+\Delta t) + u_1(t+\Delta t)\right)\left(r_1(t+\Delta t)^2 - r_0(t+\Delta t)^2\right) = b_1.$$

The value of b_1 is constant for all time. Therefore

$$u_0(t+\Delta t) = \frac{4b_1}{r_1(t+\Delta t)^2} - u_1(t+\Delta t)$$

as $r_0(t) = 0 \quad \forall\, t$.

6. Finally, the value of $u_N(t+\Delta t) = \frac{1}{5}u_0(t+\Delta t)$, from the boundary condition at $r_N \ \forall\, t$.

Results are presented in Section 4.1.

3.2   A velocity based moving mesh method for superfast diffusion

We now discuss a suitable method to model superfast diffusion in isolation. In doing this we additionally gain an appreciation of the differences in the structure of the diffusion equation, the boundary conditions, and how we must use those boundary conditions.

We assume that the inflow boundary receives an ingress of liquid mass originating from the slow diffusion regime, and so, unlike the slow diffusion method with constant mass between nodes in the mesh, we now have changing mass at each time step. We therefore make the assumption that the mass *fraction* of the total mass in the fast domain at each time step, between adjacent nodes, is constant.

If we denote the left hand boundary, which receives mass from the slow regime,by $r_I(t)$, where I represents the interface, then we put

$$r_0(t) = r_I(t).$$

The domain is then $r_I(t)$ to $r_N(t)$ for N initial equally spaced nodes in thesuperfast region.

At r_I, it is assumed that the boundary values are given by the self-similar solution $u(r,t) = u(0,t)/5$. The initial conditions are also taken to be the solutions to the self similar solution at $r_i(t)$. We start with the initial conditions

$$u_I = \frac{2}{5} \quad \text{at} \quad t_0 = 1$$

therefore from equation (8)

$$r_0 = \frac{8}{\sqrt{5}} \quad \text{at} \quad t_0 = 1.$$

Also, from the self similar solution, substituting $t_0 = 1$ into the appropriate equations

$$\left. \frac{\partial u}{\partial t} \right|_I = \frac{(r_I)^2}{8} - 1 \quad \text{at} \quad t_0,$$

and

$$\left. \frac{\partial u}{\partial r} \right|_I = -\frac{r_I}{4} \quad \text{at} \quad t_0.$$

We can also find an expression for the initial velocity of the slow/fast interface, $r_I(t)$, from

$$\left. \frac{\mathrm{d}u}{\mathrm{d}t} \right|_I = \left(\left. \frac{\partial u}{\partial r} \right|_I \middle/ \left. \frac{\mathrm{d}r}{\mathrm{d}t} \right|_I \right) + \left. \frac{\partial u}{\partial t} \right|_I .$$

Since at the interface

$$\left. \frac{\mathrm{d}u}{\mathrm{d}t} \right|_I = 0 \quad \text{at time} \quad t,$$

then the velocity at the interface node is therefore given by

$$
\begin{aligned}
\left. \frac{\mathrm{d}r}{\mathrm{d}t} \right|_I &= -\left. \frac{\partial u}{\partial t} \right|_I \middle/ \left. \frac{\partial u}{\partial r} \right|_I \\
&= \frac{r_I(t)}{2t} - \frac{4}{r_I(t)\sqrt{t}} \quad \text{at} \quad t.
\end{aligned}
\tag{13}
$$

Due to the flux into the region at $r_I(t)$ (from what is the slow diffusion regime)

$$ru\frac{\partial u}{\partial r} + ru\frac{\mathrm{d}r}{\mathrm{d}t} = 0 \quad \text{at} \quad r_I(t).$$

There is an additional boundary condition at $r_N(t)$, that maintains/drives migration

of the liquid.

$$u_b = 0.01 \quad \text{at } r_b, \quad t \geq 0.$$

The total mass in the fast domain $(r_I(t), r_b(t))$, θ_{fast}, is given by (the total area under the $u - r$ curve)

$$\int_{r_I(t)}^{r_b(t)} u r \mathrm{d}r = \theta_{fast}(t)$$

In this problem θ_{fast} varies with time, as mass travels into the *fast* diffusion region. Taking the time derivative, we obtain

$$\theta'_{fast}(t) = \frac{\mathrm{d}}{\mathrm{d}t} \int_{r_I(t)}^{r_b(t)} u r \, \mathrm{d}r$$

$$= \int_{r_I(t)}^{r_b(t)} r \frac{\partial u}{\partial t} \, \mathrm{d}r + \left[u r \frac{\mathrm{d}r}{\mathrm{d}t} \right]_{r_I(t)}^{r_b(t)}$$

$$= \int_{r_I(t)}^{r_b(t)} r \left(\frac{1}{r} \frac{\partial}{\partial r} \left(r u^m \frac{\partial u}{\partial r} \right) \right) \mathrm{d}r + \left[u r \frac{\mathrm{d}r}{\mathrm{d}t} \right]_{r_I(t)}^{r_b(t)}$$

$$= \left[r u^m \frac{\partial u}{\partial r} \right]_{r_I(t)}^{r_b(t)} + \left[u r \frac{\mathrm{d}r}{\mathrm{d}t} \right]_{r_I(t)}^{r_b(t)}$$

$$= r_b u_b \left. \frac{\partial u}{\partial r} \right|_b - r_I u_I^m \left. \frac{\partial u}{\partial r} \right|_I + r_b u_b \left. \frac{\mathrm{d}r}{\mathrm{d}t} \right|_b - r_I u_I \left. \frac{\mathrm{d}r}{\mathrm{d}t} \right|_I$$

where we know $\left. \frac{\partial u}{\partial r} \right|_I$ and $\left. \frac{\mathrm{d}r}{\mathrm{d}t} \right|_I$ from the boundary conditions, therefore

$$\theta'_{fast}(t) = r_b \left(u_b \left. \frac{\partial u}{\partial r} \right|_b + u_b \left. \frac{\mathrm{d}r}{\mathrm{d}t} \right|_b \right) - r_I \left(u_I^m \left. \frac{\partial u}{\partial r} \right|_I + u_I \left. \frac{\mathrm{d}r}{\mathrm{d}t} \right|_I \right). \tag{14}$$

The boundary conditions at r_b, for the superfast diffusion scenario are

$$u = u_b \quad \text{and} \quad u r v + u^m r u_r = 0 \quad \text{at} \quad r(t) = r_b(t), \quad t > 0,$$

where r_b is the far right boundary in the superfast diffusion regime. The first term in equation (14) goes to zero, therefore

$$\theta'_{fast}(t) = -r_I \left(u_I^m \left(\frac{\partial u}{\partial r} \right) \bigg|_I + u_I \left(\frac{\mathrm{d}r}{\mathrm{d}t} \right) \bigg|_I \right) \quad \text{for all} \quad t > 0. \tag{15}$$

In order to calculate the mass fractions in the fast regime, we must first obtain the

integrals of u from $r_0(t)$ to $r_i(t)$, where $i = I(= 0), 1, \ldots, N$, for N equally spaced discretisations at t_0. We divide this integral by the total mass at t_0, $\theta_{fast}(t_0)$, between r_I and $r_b(= r_N)$, to obtain the mass fraction (μ_i),

$$\mu_i = \frac{1}{\theta_{fast}(t)} \int_{r_I(t)}^{r_i(t)} ur \, dr, \tag{16}$$

where

$$\theta_{fast}(t) = \int_{r_I(t)}^{r_b(t)} ur \, dr. \tag{17}$$

The total mass θ_{fast} varies with time, as flux enters at the boundary $r_I(t)$. From equation (16)

$$\begin{aligned}
\frac{d}{dt} \int_{r_I(t)}^{r_i(t)} ur \, dr &= \frac{d}{dt} \left(\theta_{fast}(t) \mu_i \right) \\
&= \theta'_{fast}(t) \mu_i \tag{18}
\end{aligned}$$

Evaluating the left hand side of equation (18) for a general point $r_i(t)$, using Leibnitz' Rule,

$$\begin{aligned}
\theta'_{fast}(t) \mu_i &= \int_{r_I(t)}^{r_i(t)} r \frac{\partial u}{\partial t} \, dr + \left[ur \frac{dr}{dt} \right]_{r(t)}^{r_i(t)} \\
&= \int_{r_I(t)}^{r_i(t)} r \left(\frac{1}{r} \frac{\partial}{\partial r} \left(ru^m \frac{\partial u}{\partial r} \right) \right) dr + \left[ur \frac{dr}{dt} \right]_{r_I(t)}^{r_i(t)} \\
&= \left[ru^m \frac{\partial u}{\partial r} \right]_{r_I(t)}^{r_i(t)} + \left[ur \frac{dr}{dt} \right]_{r_I(t)}^{r_i(t)} \\
&= r_i(u_i)^m \left. \left(\frac{\partial u}{\partial r} \right) \right|_i - r_I(u_I)^m \left. \left(\frac{\partial u}{\partial r} \right) \right|_I + u_i r_i \left. \left(\frac{dr}{dt} \right) \right|_i - u_I r_I \left. \left(\frac{dr}{dt} \right) \right|_I.
\end{aligned}$$

So,

$$\begin{aligned}
r_i(u_i)^m \left. \frac{\partial u}{\partial r} \right|_i - r_I(u_I)^m \left. \frac{\partial u}{\partial r} \right|_I + u_i r_i \left. \frac{dr}{dt} \right|_i - u_I r_I \left. \frac{dr}{dt} \right|_I &= \theta'_{fast}(t) \mu_i \\
&= -r_I \left((u_I)^m \left. \frac{\partial u}{\partial r} \right|_I + u_I \left. \frac{dr}{dt} \right|_I \right) \mu_i
\end{aligned}$$

from the definition of $\theta'_{fast}(t)$, equation (15).

Rearranging to obtain a velocity for the spatial nodes in the superfast regime mesh,

21

at time t, we obtain

$$\left.\frac{\mathrm{d}r}{\mathrm{d}t}\right|_i = \left(\frac{u_I r_I}{u_i r_i}\right)(1-\mu_i)\left.\frac{\mathrm{d}r}{\mathrm{d}t}\right|_I + \left(\frac{(u_I)^m r_I}{u_i r_i}\right)(1-\mu_i)\left.\frac{\partial u}{\partial r}\right|_I - (u_i)^{m-1}\left.\frac{\partial u}{\partial r}\right|_i. \qquad (19)$$

Hence, calculating the velocity of the internal nodes at any time requires knowledge of the boundary values at r_I, i.e, u_I, $\left.\frac{\mathrm{d}r}{\mathrm{d}t}\right|_I$ and $\left.\frac{\partial u}{\partial r}\right|_I$, making use of the self similar solution. Using the previous equation (13), to recap

$$\left.\frac{\mathrm{d}r}{\mathrm{d}t}\right|_I = \frac{r_I}{2t} - \frac{4}{r_I\sqrt{t}} \quad \text{at time } t$$

and from our knowledge at the interface,

$$\left.\frac{\partial u}{\partial r}\right|_I = -\frac{r_I}{4t} \quad \text{and} \quad \left.\frac{\partial u}{\partial t}\right|_I = \frac{(r_I)^2}{8t^2} - \frac{1}{t^{3/2}},$$

we can substitute these into expressions into equation (19) to obtain

$$\left.\frac{\mathrm{d}r}{\mathrm{d}t}\right|_i = \left(\frac{u_I r_I}{u_i r_i}\right)(1-\mu_i)\left(\frac{r_I}{2t} - \frac{4}{r_I\sqrt{t}}\right) + \left(\frac{(u_I)^m r_I}{u_i r_i}\right)(1-\mu_i)\left(-\frac{r_I}{4t}\right) - (u_i)^{m-1}\left.\left(\frac{\partial u}{\partial r}\right)\right|_i.$$

This is how the velocity of the spatial nodes, $r(t)$ progress in the superfast diffusion domain.

We now seek a suitable time-stepping method for the superfast moving mesh method, and update the position of each spatial node r_i by

$$r_i(t+\Delta t) = r_i(t) + \Delta t \left.\frac{\mathrm{d}r}{\mathrm{d}t}\right|_i,$$

and the total mass $\theta_{fast}(t+\Delta t)$ by

$$\theta_{fast}(t+\Delta t) = \theta_{fast}(t) + \Delta t \theta'_{fast}(t),$$

where $\theta'_{fast}(t)$ is given by equation (15). We have expressions for both $\left.\frac{\partial u}{\partial r}\right|_I$ and $\left.\frac{\mathrm{d}r}{\mathrm{d}t}\right|_I$ (derived from the self similar solution). So equation (15) becomes

$$\theta'_{fast}(t) = \left\{\frac{(r_I)^2 u_I}{2t}\left(\frac{(u_I)^{m-1}}{2} - 1\right)\right\} + \left(\frac{4u_I}{\sqrt{t}}\right). \qquad (20)$$

We can now recover the solution for $u(r(t+\Delta t), t+\Delta t)$ at the next time step, approx-

imating equation (16) as

$$u_i(t + \Delta t) = \theta_{fast}(t + \Delta t) \frac{\mu_{i+1} - \mu_{i-1}}{r_i(t + \Delta t)\,(r_{i+1}(t + \Delta t) - r_{i-1}(t + \Delta t))}. \qquad (21)$$

The individual mass fractions (μ_i) do not change with time. The self similar solution is used to calculate values of $u(r, t)$ and the velocities of the spatial nodes, v_i at time $t = 0$, at what would be the boundary with the slow diffusion regime.

In the superfast region we can no longer use the self-similar solution, and fit a parabola between the final node of the self similar solution/slow parabola, and the final node in the superfast diffusion profile, where we have assigned a finite value of $u(N, t) = 0.01$. We give the solution at the final node this small value of u in order to ensure the advancement of the fluid. In reality, where $u(N, t) = 0$ the capillary bridges in Figure 3 would collapse and no longer exist, and therefore there would be no further fluid advancement through the porous medium. The fluid would just coat the surface roughness, and only be in contact with individual particles. Migration then eventually stops.

We use the last value in the self similar solution to get $\frac{dr}{dt}\big|_I$ at any time t.

3.3 Setting up the initial superfast profile using a quadratic.

At initial time, $t_0 = 1$, we have values for the velocity, $\frac{dr}{dt}\big|_I = v_I$ at r_I, and the concentration $u_I(t)$ from the self similar / parabola solution. We select an initial spatial step size Δr, and the number of steps N. We then apply the boundary condition

$$u_N(t) = 0.01 \quad \text{at} \quad r_N = r_I + (N\Delta r)$$

at initial time t_0. We can generate the shape for the initial $u(r, t_0)$ profile by applying a parabola between

$$u_I(t_0) = \frac{2}{5} \quad \text{at} \quad r_I(t_0) = \frac{8}{\sqrt{5}}.$$

This will enable us to calculate the values $u_i(t_0)$, thus enabling the calculation of all the mass fractions between $r_I(t_0)$ and $r_i(t_0)$, (μ_i) which remain constant for $t > 0$.

The initial values of $u_i(t_0)$ in the fast diffusion regime are given by

$$u_i = u_N + (u_I - u_N)\left(\frac{N\Delta r + r_I - r_i}{(N\Delta r)^2}\right). \tag{22}$$

The total mass in the fast region, at t_0 is therefore given by

$$\theta_{fast} = \int_{r_I}^{r_I+N\Delta r} ur\,\mathrm{d}r \quad \text{at } t_0,$$

which can be calculated using Simpson's Rule. The mass fractions, μ_i are given by,

$$\mu_i = \frac{\theta_i(t_0)}{\theta_{fast}(t_0)},$$

where

$$\theta_i = \int_{r_I}^{r_I+i\Delta r} ur\,\mathrm{d}r \quad \text{at} \quad t_0.$$

At any time t, the mass from position $r_I(t)$ to position $r_i(t)$ is given by

$$\theta_i(t) = \mu_i\theta_{fast}(t)$$

where $\theta_{fast}(t)$ is derived using equation 17. Values of $\theta_i(t)$ are then used to calculate the values of $u_i(t + \Delta t)$ using equation (21).

3.4 Algorithm for the superfast diffusion regime using constant mass fractions

We can progress the superfast diffusion region in isolation following discretisation of the mesh at t_0, $r_i(t)$. The solution values for $u_i(r_i, t)$ (at time t_0) from the parabolic initial profile) are calculated using the following algorithm. Initially:

1. For a domain $r_I(t_0), r_b(t)$, uniformly discretise the mesh using a spacing Δr

$$r_i = i\Delta r + r_I \quad \text{at} \quad t_0 = 1.$$

2. Define the initial values at $t_0 = 1$

$$u_I = \frac{2}{5}, \quad r_I = 8/\sqrt{5}, \quad \left.\frac{\mathrm{d}r}{\mathrm{d}t}\right|_I = v_I = \frac{r_I}{2} - \frac{4}{r_I} \quad \text{at } t_0.$$

24

3. Define the boundary conditions at $r_I(t)$ at time t

$$u_I = \frac{2}{\sqrt{t}} - \frac{r_I}{8t}, \quad \text{as given by the self similar solution}$$

$$v_I = \frac{r_I}{2t}\bigg|_I - \frac{4}{r_I\sqrt{t}}, \quad \text{as given by the self similar solution}$$

4. Define the boundary conditions at $r_b(t)$

$$u_b = 0.01, \quad u_b^m r_b \frac{\partial u}{\partial r}\bigg|_b + u_b r_b \frac{\mathrm{d}r}{\mathrm{d}t}\bigg|_b = 0.$$

5. Calculate the initial total mass under the superfast parabola using Simpson's Rule.

$$\theta_{fast} = \int_{r_I}^{r_b} ur\,\mathrm{d}r \quad \text{at} \quad t_0,$$

and, additionally the masses between r_I and r_i, $i = I, 2, \ldots, N$,

$$\theta_i = \int_{r_I}^{r_i} ur\,\mathrm{d}r \quad \text{at} \quad t_0$$

6. Then compute the mass fractions, μ_i, $i = I, 2, \ldots, N$,

$$\mu_i = \frac{\theta_i}{\theta_{fast}} \quad \text{at} \quad t_0.$$

Then, at each time step,

1. Calculate the velocity of the internal nodes, $v_I(t)$ using the expression derived from the constant mass fraction approach, using previous equation (19).

2. Calculate the velocity of the end node at time t, $v_b(t)$ using linear extrapolation, utilising the calculated velocities for the previous two spatial nodes at t,

$$v_N \left(= \frac{\mathrm{d}r}{\mathrm{d}t}\bigg|_N \right) = 2v_{N-1} - v_{N-2}, \quad \text{where N is the number of discretisations.}$$

3. Update the position vector of the Ith node at $t + \Delta t$, using the velocity of the previous node, $v_i(t)$ and the explicit Euler method.

$$r_i(t + \Delta t) = r_i(t) + v_i(t)\Delta t, \quad i = 2, \ldots, N$$

4. Compute the new total mass from $r_I(t+\Delta t)$ to $r_N(t+\Delta t)$ using $\theta'_{fast}(t)$ calculated from Equation (20), and explicit Euler method.

$$\theta_{fast}(t + \Delta t) = \theta_{fast}(t) + (\theta'_{fast}(t))\Delta t$$

5. Calculate the new partial masses from $r_I(t + \Delta t)$ to $r_i(t + \Delta t)$ using

$$\theta_i(t + \Delta t) = \mu_i \theta_{fast}(t + \Delta t).$$

6. Use the new total partial masses, $\theta_i(t + \Delta t)$ to calculate the updated values of $u_i(t + \Delta t)$ using the previous equation (21) for $i = 2, \ldots, N - 1$.

7. Calculate $u_I(t + \Delta t)$ using the self similar solution equation (8). The boundary conditions specify that $u_N(t + \Delta t) = 0.01$, for all t.

3.5 Moving mesh generation for slow diffusion with constant mass fractions.

We now re-address the moving mesh method for the slow diffusion, $m = 1$ in equation (1), but in the case where there is a loss of mass overall, as mass moves out of the domain (into the superfast). We must therefore, as in the previous section for fast diffusion, adopt the use of constant mass fractions between spatial nodes.

We discretise the r axis up to the point $r_I(t)$. It is at this point that we will, in the next section, attach the superfast diffusion regime. For the domain $(r_0(t), r_I(t))$

$$r_i = r_0 + i\Delta r \quad i = 0, \ldots, I$$

where $r_0 = 0$ at the origin, and I is the number of equally spaced spatial discretisations. The self-similar solution/new parabola is then used to calculate the values $u_i(t)$ at initial time $t_0 = 1$ up to the interface with the superfast regime at $u_I = \frac{1}{5}u_0$, as in the case of the slow regime with mass conservation.

$$u_i = 2 - \frac{r_i^2}{8}, \quad \text{at } t_0$$

The boundary conditions at $r_0 = 0$, $t_0 = 1$ are

$$
\begin{aligned}
u_0 &= 2, \\
\left. \frac{\partial u}{\partial r} \right|_0 &= 0, \\
\left. \frac{\mathrm{d}r}{\mathrm{d}t} \right|_0 &= 0,
\end{aligned}
$$

and for all time $t > 0$,

$$
\left. \frac{\partial u}{\partial r} \right|_0 = 0,, \tag{23}
$$

$$
\left. \frac{\mathrm{d}r}{\mathrm{d}t} \right|_0 = 0,, \tag{24}
$$

as, intuitively, the origin about which diffusion is symmetric, $r_0(t) = 0$.

Let us denote the position and solution at the interface between slow and superfast diffusion as r_I and u_I respectively, at t_0, where I is the spatial nodal identity. We know from previous equations (25), (26), (27), and (28) respectively, that at $t_0 = 1$ for an initial discretisation $\Delta r = \frac{1}{4\sqrt{5}}$,

$$
r_I = \frac{8}{\sqrt{5}}, \tag{25}
$$

$$
\left. \frac{\partial u}{\partial r} \right|_I = -\frac{2}{\sqrt{5}}, \tag{26}
$$

$$
\left. \frac{\mathrm{d}r}{\mathrm{d}t} \right|_I = \frac{3\sqrt{5}}{10}, \tag{27}
$$

$$
\left. \frac{\partial u}{\partial t} \right|_I = \frac{3}{5}. \tag{28}
$$

However we now only use the value of r_I at time t_0. The initial total mass in the slow region at t_0 is calculated for the integral

$$
\theta_{slow}(t_0) = \int_{r_0}^{r_I} ur \, \mathrm{d}r
$$

The rate of change of mass $\theta'_{slow}(t)$ overall in the region can calculated at time t using

Leibnitz' Integral Rule

$$
\begin{aligned}
\theta'_{slow}(t) &= \frac{\mathrm{d}}{\mathrm{d}t} \int_{r_0(t)}^{r_I(t)} ur \mathrm{d}r \\
&= \int_{r_0(t)}^{r_I(t)} r\frac{\partial u}{\partial t}\mathrm{d}r + \left[ur\frac{\mathrm{d}r}{\mathrm{d}t} \right]_{r_0(t)}^{r_I(t)} \\
&= \int_{r_0(t)}^{r_I(t)} r\left(\frac{1}{r}\left(\frac{\partial}{\partial t}ur\frac{\partial u}{\partial r} \right) \right)\mathrm{d}r + \left[ur\frac{\mathrm{d}r}{\mathrm{d}t} \right]_{r_0(t)}^{r_I(t)} \\
&= \left[ur\frac{\partial u}{\partial r} \right]_{r_0(t)}^{r_I(t)} + \left[ur\frac{\mathrm{d}r}{\mathrm{d}t} \right]_{r_0(t)}^{r_I(t)} \\
&= u_I(t)r_I(t)\left(\frac{\partial u}{\partial r} \right)\bigg|_I + u_I(t)r_I(t)\left(\frac{\mathrm{d}r}{\mathrm{d}t} \right)\bigg|_I .
\end{aligned}
\tag{29}
$$

and equations (23) and (24) from the boundary conditions at $r_0(t)$. If we consider a general point $r_i(t)$ in the slow diffusion domain, then the mass fraction, μ_i of the total mass from r_0 to r_I is given by

$$
\frac{1}{\theta_{slow}(t)} \int_{r_0(t)}^{r_i(t)} ur \mathrm{d}r = \mu_i \quad i = 0, \ldots, I,
$$

which is constant for all time. Therefore the rate of change of mass between r_0 and r_i at time t is given by

$$
\frac{\mathrm{d}}{\mathrm{d}t} \int_{r_0(t)}^{r_i(t)} ur\,\mathrm{d}r = \theta'_{slow}(t)\mu_i,
$$

and, by Leibnitz Integral Rule,

$$
\frac{\mathrm{d}}{\mathrm{d}t} \int_{r_0(t)}^{r_i(t)} ur\,\mathrm{d}r = \int_{r_0(t)}^{r_i(t)} r\frac{\partial u}{\partial t}\,\mathrm{d}r + \left[ur\frac{\mathrm{d}r}{\mathrm{d}t} \right]_{r_0(t)}^{r_i(t)} .
$$

Therefore,

$$
u_i r_i\left(\frac{\mathrm{d}r}{\mathrm{d}t} \right)\bigg|_i - u_0 r_0\left(\frac{\mathrm{d}r}{\mathrm{d}t} \right)\bigg|_0 + u_i r_i\left(\frac{\partial u_i}{\partial r_i} \right)\bigg|_i - r_0 u_0\left(\frac{\partial u}{\partial r} \right)\bigg|_0 = \theta'_{slow}(t)\mu_i .
$$

Substituting in equation (29) for $\theta'_{slow}(t)$, we obtain

$$
u_i r_i\left(\frac{\mathrm{d}r}{\mathrm{d}t}\bigg|_i + \frac{\partial u}{\partial r}\bigg|_i \right) - u_0 r_0\left(\frac{\mathrm{d}r}{\mathrm{d}t}\bigg|_0 + \frac{\partial u}{\partial r}\bigg|_0 \right) = u_I r_I \mu_i\left(\frac{\mathrm{d}r}{\mathrm{d}t}\bigg|_I + \frac{\partial u}{\partial r}\bigg|_I \right)
$$

Therefore, since

$$\frac{dr}{dt}\bigg|_0 = 0 \quad \text{and} \quad \frac{\partial u}{\partial r}\bigg|_0 = 0 \quad \text{at} \quad r_0(t) = 0$$

$$\frac{dr}{dt}\bigg|_i = \frac{u_I r_I \mu_i}{u_i r_i}\left(\frac{\partial u}{\partial r}\bigg|_I + \frac{dr}{dt}\bigg|_I\right) - \frac{\partial u}{\partial r}\bigg|_i \quad \text{at time } t, \tag{30}$$

for nodes/positions r_0 to r_{I-1}.

It is now necessary to identify $\frac{\partial u}{\partial r}\big|_I$ and $\frac{dr}{dt}\big|_I$ at the interface, at time t, and can approximate them using central differences

$$\frac{\partial u}{\partial r}\bigg|_I \approx \frac{u_{I+1} - u_{I-1}}{r_{I+1} - r_{I-1}} \quad \text{at time } t,$$

and

$$\frac{\partial u}{\partial r}\bigg|_i \approx \frac{u_{i+1} - u_{i-1}}{r_{i+1} - r_{i-1}} \quad \text{at time } t,$$

or by one sided differences

$$\frac{\partial u}{\partial r}\bigg|_I \approx \frac{u_I - u_{I-1}}{r_I - r_{I-1}} \quad \text{or} \quad \frac{\partial u}{\partial r}\bigg|_I \approx \frac{u_{I+1} - u_I}{r_{I+1} - r_I},$$

and

$$\frac{\partial u}{\partial r}\bigg|_i \approx \frac{u_i - u_{i-1}}{r_i - r_{i-1}} \quad \text{or} \quad \frac{\partial u}{\partial r}\bigg|_i \approx \frac{u_{i+1} - u_i}{r_{i+1} - r_i}.$$

The velocity of the nodes in the fast regime are calculated using equation (19) derived in Section (3.2). The velocity of the interface node, $\frac{dr}{dt}\big|_I$ is calculated from consideration of a zero rate of change of flux across the interface between the slow and superfast regimes, which we shall describe in the next section.

3.6 Calculating the velocity of the interface node, $v_I(t)$ for the combined slow and superfast diffusion

In this section we derive a method to calculate the velocity of the spatial node at the interface between slow and superfast diffusion. We consider the area under the plot of u against r at time t, between r_{I-1} and r_I in the slow regime, and between r_I and r_{I+1} in the superfast regime. The interface is shown in Figure 6.
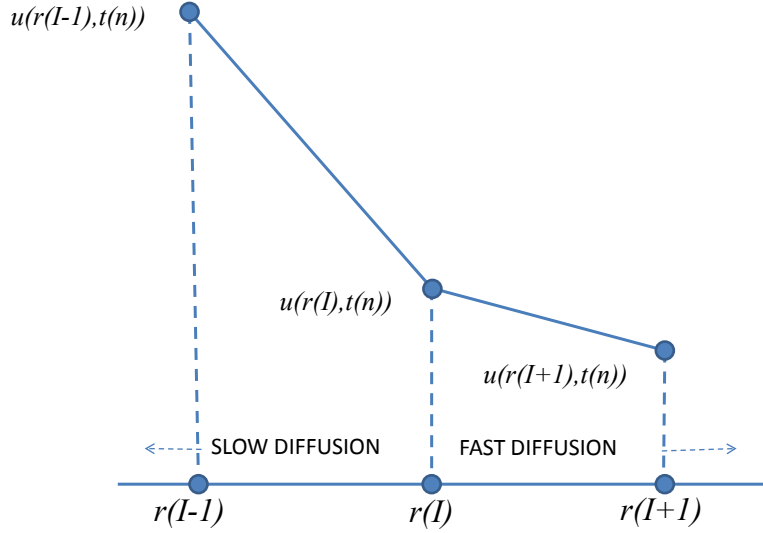
Figure 6: Identification of velocity of interface node between slow and fast diffusion regimes

There will be zero rate of change of mass as mass flows at the same rate into the superfast regime as flows out of the slow regime, by the application of the continuity equation at the boundary;

$$\frac{\mathrm{d}}{\mathrm{d}t}\left(\frac{1}{\theta_{slow(1)}}\int_{r_{I-1}(t)}^{r_I(t)} ur\,\mathrm{d}r + \frac{1}{\theta_{fast(1)}}\int_{r_I(t)}^{r_{I+1}(t)} ur\,\mathrm{d}r\right) = 0. \tag{31}$$

where $\theta_{slow(1)}$ and $\theta_{fast(1)}$ represent the total mass in the slow and fast regimes respectively at time t_0. The integral to the left of the boundary is given by

$$\begin{aligned}
\frac{\mathrm{d}}{\mathrm{d}t}\frac{1}{\theta_{slow(1)}}\int_{r_{I-1}}^{r_I} ur\,\mathrm{d}r &= \frac{1}{\theta_{slow(1)}}\left(\int_{r_{I-1}}^{r_I}\frac{\partial u}{\partial t}r\,\mathrm{d}r + \left[ur\frac{\mathrm{d}r}{\mathrm{d}t}\right]_{I-1}^{I}\right)\\
&\quad - \frac{1}{(\theta_{slow(1)})^2}\frac{\mathrm{d}\theta_{slow(1)}}{\mathrm{d}t}\int_{r_{I-1}}^{r_I} ur\,\mathrm{d}r,
\end{aligned} \tag{32}$$

30

and to the right it is

$$\frac{\mathrm{d}}{\mathrm{d}t}\frac{1}{\theta_{fast(1)}}\int_{r_I}^{r_{I+1}} ur\,\mathrm{d}r \;=\; \frac{1}{\theta_{fast(1)}}\left(\int_{r_I}^{r_{I+1}}\frac{\partial u}{\partial t}r\,\mathrm{d}r + \left[ur\frac{\mathrm{d}r}{\mathrm{d}t}\right]_I^{I+1}\right)$$

$$-\;\frac{1}{(\theta_{fast(1)})^2}\frac{\mathrm{d}\theta_{fast(1)}}{\mathrm{d}t}\int_{r(I)}^{r(I+1)} ur\,\mathrm{d}r. \qquad (33)$$

Within equation (32),

$$\int_{r_{I-1}}^{r_I}\frac{\partial u}{\partial t}r\,\mathrm{d}r + \left[ur\frac{\mathrm{d}r}{\mathrm{d}t}\right]_{I-1}^I \;=\; \int_{r_{I-1}}^{r_I} r\left(\frac{1}{r}\left(\frac{\partial}{\partial r}ur\frac{\partial u}{\partial r}\right)\right)\mathrm{d}r + \left[ur\frac{\mathrm{d}r}{\mathrm{d}t}\right]_{r_{I-1}}^{r_I}$$

$$=\; \left[ur\frac{\partial u}{\partial r}\right]_{r_{I-1}}^{r_I} + \left[ur\frac{\mathrm{d}r}{\mathrm{d}t}\right]_{r_{I-1}}^I$$

$$=\; u_I r_I\left(\left.\frac{\partial u}{\partial r}\right|_I + \left.\frac{\mathrm{d}r}{\mathrm{d}t}\right|_I\right)$$

$$-\; u_{I-1} r_{I-1}\left(\left.\frac{\partial u}{\partial r}\right|_{I-1} + \left.\frac{\mathrm{d}r}{\mathrm{d}t}\right|_{I-1}\right), \qquad (34)$$

for slow diffusion, and for the superfast diffusion, within equation (33),

$$\int_{r_I}^{r_{I+1}}\frac{\partial u}{\partial t}r\,\mathrm{d}r + \left[ur\frac{\mathrm{d}r}{\mathrm{d}t}\right]_I^{I+1} \;=\; \int_{r_I}^{r_{I+1}} r\left(\frac{1}{r}\left(\frac{\partial}{\partial r}u^m r\frac{\partial u}{\partial r}\right)\right)\mathrm{d}r + \left[ur\frac{\mathrm{d}r}{\mathrm{d}t}\right]_{r_I}^{r_{I+1}}$$

$$=\; \left[u^m r\frac{\partial u}{\partial r}\right]_{r_I}^{r_{I+1}} + \left[ur\frac{\mathrm{d}r}{\mathrm{d}t}\right]_{r_I}^{r_{I+1}}$$

$$=\; u_{I+1} r_{I+1}\left(\left.u_{I+1}^{m-1}\frac{\partial u}{\partial r}\right|_{I+1} + \left.\frac{\mathrm{d}r}{\mathrm{d}t}\right|_{I+1}\right)$$

$$-\; u_I^m r_I\left(\left.\frac{\partial u}{\partial r}\right|_I + \left.\frac{\mathrm{d}r}{\mathrm{d}t}\right|_I\right). \qquad (35)$$

We have expressions for both the velocity of the penultimate node in the slow region $\left.\frac{\mathrm{d}r}{\mathrm{d}t}\right|_{I-1}$ and the velocity of the second node in the superfast region, after the interface, $\left.\frac{\mathrm{d}r}{\mathrm{d}t}\right|_{I+1}$ defined previously

$$\left.\frac{\mathrm{d}r}{\mathrm{d}t}\right|_{I-1} = \frac{u_I r_I \mu_{I-1}}{u_{I-1} r_{I-1}}\left(\left.\frac{\partial u}{\partial r}\right|_I + \left.\frac{\mathrm{d}r}{\mathrm{d}t}\right|_I\right) - \left.\frac{\partial u}{\partial r}\right|_{I-1},$$

and

$$\left.\frac{\mathrm{d}r}{\mathrm{d}t}\right|_{I+1} = \frac{u_I r_I}{u_{I+1} r_{I+1}}(1-\mu_{I+1})\left.\frac{\mathrm{d}r}{\mathrm{d}t}\right|_I + \frac{u_I^m r_I}{u_{I+1} r_{I+1}}(1-\mu_{I+1})\left.\frac{\partial u}{\partial r}\right|_I - u_{I+1}^{m-1}\left.\frac{\partial u}{\partial r}\right|_{I+1},$$

from equations (30) and (19) respectively. So, substituting equations (32), (33) (34) (35)into equation (31), the following expression is obtained for equation (31)

$$
\begin{aligned}
0 = & \frac{1}{\theta_{slow(1)}} \left(u_I r_I \left(\frac{\partial u}{\partial r}\bigg|_I + \frac{dr}{dt}\bigg|_I \right) - u_{I-1} r_{I-1} \left(\frac{\partial u}{\partial r}\bigg|_{I-1} + \frac{dr_{I-1}}{dt}\bigg|_{I-1} \right) \right) \\
& - \frac{1}{(\theta_{slow(1)})^2} \frac{d\theta_{slow(1)}}{dt} \int_{r_{I-1}(t)}^{r_I(t)} u r \, dr \\
& + \frac{1}{\theta_{fast(1)}} \left(u_{I+1} r_{I+1} \left(u_{I+1}^{m-1} \frac{\partial u}{\partial r}\bigg|_{I+1} + \frac{dr}{dt}\bigg|_{I+1} \right) - u_I r_I \left(u_I^{m-1} \frac{\partial u}{\partial r}\bigg|_I + \frac{dr}{dt}\bigg|_I \right) \right) \\
& - \frac{1}{(\theta_{fast(1)})^2} \frac{d\theta_{fast(1)}}{dt} \int_{r_I(t)}^{r_{I+1}(t)} u r \, dr.
\end{aligned} \tag{36}
$$

Following substitution of equations (30) for $\frac{dr}{dt}\big|_{I-1}$ and (19) for $\frac{dr}{dt}\big|_{I+1}$,

$$
\begin{aligned}
0 = & \frac{u_I r_I}{\theta_{slow(1)}} \left(1 - \mu_{I-1} + \frac{(u_I + u_{I-1})(r_I^2 - r_{I-1}^2)}{4\theta_{slow(1)}} \right) \frac{\partial u}{\partial r}\bigg|_I \\
& + \left[\frac{u_I r_I}{\theta_{slow(1)}} \left(1 - \mu_{I-1} + \frac{(u_I + u_{I-1})(r_I^2 - r_{I-1}^2)}{4\theta_{slow(1)}} \right) \right] \frac{dr}{dt}\bigg|_I \\
& + \left[\frac{u_I r_I}{\theta_{fast(1)}} \left(\mu_{I+1} + \frac{(u_{I+1} + u_I)(r_{I+1}^2 - r_I^2)}{4\theta_{fast(1)}} \right) \right] \frac{dr}{dt}\bigg|_I \\
& + \frac{u_I r_I}{\theta_{fast(1)}} \left(1 - \mu_{I+1} + \frac{(u_{I+1} + u_I)(r_{I+1}^2 - r_I^2)}{4\theta_{fast(1)}} \right) \frac{\partial u}{\partial r}\bigg|_I,
\end{aligned}
$$

where, in equation (36),

$$
\begin{aligned}
\frac{1}{(\theta_{slow(1)})^2} \frac{d\theta_{slow(1)}}{dt} \int_{r_{I-1}(t)}^{r_I(t)} u r \, dr & = \frac{1}{(\theta_{slow(1)})^2} \theta'_{slow}(t) \frac{(r_I^2 - r_{I-1}^2)(u_I + u_{I-1})}{4} \\
& = \frac{(r_I^2 - r_{I-1}^2)(u_I + u_{I-1})}{4(\theta_{slow(1)})^2} u_I r_I \left(\frac{\partial u}{\partial r}\bigg|_I + \frac{dr}{dt}\bigg|_I \right)
\end{aligned}
$$

and

$$
\frac{1}{(\theta_{fast(1)})^2} \frac{d\theta_{fast(1)}}{dt} \int_{r_I(t)}^{r_{I+1}(t)} u r \, dr = -\frac{u_I r_I (r_{(I+1)}^2 - r_I^2)(u_{I+1} + u_I)}{4(\theta_{fast(1)})^2} \left(u_I^{m-1} \frac{\partial u}{\partial r}\bigg|_I + \frac{dr}{dt}\bigg|_I \right)
$$

We therefore obtain an expression for the velocity of the interface node $\frac{dr}{dt}\big|_I$

$$
\frac{dr}{dt}\bigg|_I = \frac{-(\partial u_I^n / \partial r_I^n)A}{B} \tag{37}
$$

32

where

$$
\begin{aligned}
A &= \frac{u_I r_I}{\theta_{slow(1)}} \left(1 - \mu_{I-1} - \frac{(r_I^2 - r_{I-1}^2)(u_I + u_{I-1})}{4\theta_{slow(1)}} \right) \\
&+ \frac{u_I^m r_I}{\theta_{fast(1)}} \left(\frac{(r_{I+1}^2 - r_I^2)(u_{I+1} + u_I)}{4\theta_{fast(1)}} - \mu_{I+1} \right)
\end{aligned}
$$

and

$$
\begin{aligned}
B &= \frac{u_I r_I}{\theta_{slow(1)}} \left(1 - \mu_{I-1} - \frac{(r_I^2 - r_{I-1}^2)(u_I + u_{I-1})}{4\theta_{slow(1)}} \right) \\
&+ \frac{u_I r_I}{\theta_{fast(1)}} \left(\frac{(r_{I+1}^2 - r_I^2)(u_{I+1} + u_I)}{4\theta_{fast(1)}} - \mu_{I+1} \right)
\end{aligned}
$$

3.7 Combining the initial profile for slow and fast diffusive regimes at initial time t_0.

Now that we have expressions for the velocity of the spatial nodes in the slow diffusion regime, equation (30), the superfast regime, equation (19) and the interface velocity, equation (37), we can now model the combined diffusion scenario.

For initial profile at t_0, the change in diffusion equation, where there is a change in the value of m from 1 to $-\frac{3}{2}$, can be seen at $r(t_0) = \frac{8}{\sqrt{5}}$ (Figure 7). The self similar solution parabola is used for the slow diffusion profile at t_0, equation (8), and this is attached to the superfast parabola, given by equation (22).
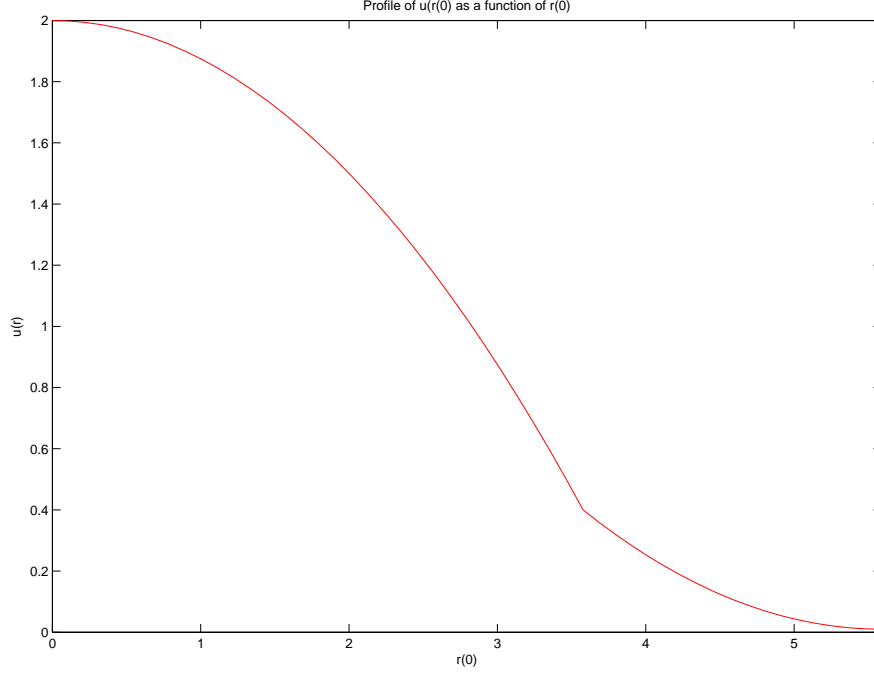
Figure 7: Combined slow and fast diffusion profiles at t_0.

3.8 Generating an algorithm for the combined diffusion.

We now generate an algorithm to advance the initial profile described in Section (3.7).

Combining slow and superfast diffusion

For a mesh r_i, $i = 0, \ldots, N$,

$$0 = r_0(t) < r_i(t) < \ldots < r_I < \ldots < r_{N-1}(t) < r_N(t)$$

which is uniform at t_0, with N nodes a distance Δr apart, $r_N(t)$ being a moving boundary. The interface node, $r_I(t)$ is the node at which the slow diffusion regime changes to the superfast regime.

Initially

1. At t_0, and given the boundary condition

$$u_N(t) = 0.01,$$

34

for all t, calculate the initial solutions $u_i(t_0)$:

$$u_i = 2 - \frac{r_i^2}{8}, \quad 0 \le r_i \le r_I, \quad i = 0, \ldots, I.$$

$$u_i = u_N + (u_I - u_N)\left(\frac{N\Delta r + r_I - r_i}{(N\Delta r)^2}\right), \quad r_I \le r_i \le r_{N-1}, \quad i = I, \ldots, N.$$

2. At r_0, the velocity $v_0(t) = 0$, for all t

3. Calculate the initial total masses in both regions, as described in Sections 3.5 and 3.2 for slow ($\theta_{slow(1)}$) and fast ($\theta_{fast(1)}$) diffusion respectively,

$$\theta_{slow}(t_0) = \int_{r_0}^{r_I} ur \, dr,$$

$$\theta_{fast}(t_0) = \int_{r_I}^{r_N} ur \, dr,$$

4. Calculate the overall initial total mass M_{tot}, which is constant in time

$$M_{tot} = \theta_{slow}(t_0) + \theta_{fast}(t_0)$$

5. Calculate the individual initial masses, $\theta_i(t_0)$ for both the slow and fast diffusion.

$$\theta_i(t_0) = \int_{r_0}^{r_i} ur \, dr, \quad i = 0, \ldots, I. \quad \text{for slow diffusion}$$

$$\theta_i(t_0) = \int_{r_I}^{r_i} ur \, dr, \quad i = I, \ldots, N. \quad \text{for fast diffusion}$$

6. Calculate the individual , constant mass fraction (μ_i) for both slow and fast diffusion regions from the information at t_0 for $\theta_i(t_0)$,

$$\mu_i = \frac{\theta_i(t_0)}{\theta_{slow(1)}}, \quad \text{for slow diffusion}, \quad i = 0, \ldots, I$$

$$\mu_i = \frac{\theta_i(t_0)}{\theta_{fast(1)}}, \quad \text{for fast diffusion}, \quad i = I, \ldots, N.$$

Then, for each time step,

1. Calculate the velocity, v_I of the interface node at r_I using equation (37) in Section (3.6),

2. Calculate the velocity v_i of the spatial nodes in the slow diffusion regime using equation (30) in Section 3.5 for $i = 1, \ldots, I - 1$.

3. Calculate the velocity v_i of the spatial nodes in the superfast diffusion regime using equation (19) in Section 3.2 for $i = I + 1, \ldots, N - 1$.

4. Calculate the final velocity using linear interpolation at time t_0

$$v_N = 2v_{N-1} - v_{N-2}$$

5. Calculate the updated mesh position at $t + \Delta t$, where Δt is the time increment, which is constant for all time, using explicit Euler time stepping.

$$r_i(t + \Delta t) = r_i(t) + \Delta t v_i(t), i = 1, \ldots, N$$

6. Calculate the updated mass in the slow diffusion regime, $\theta_{slow}(t + \Delta t)$, using equation (29) to obtain the rate of change of mass (in the slow region)

$$\theta_{slow}(t + \Delta t) = \theta'_{slow}(t)\Delta t + \theta_{slow}(t)$$

7. Update the mass in the superfast diffusion regime at time $t + \Delta t$

$$\theta_{fast}(t + \Delta t) = M_{tot} - \theta_{slow}(t + \Delta t)$$

as the total mass across the combined domain is constant for all time.

8. Calculate the updated solution values u_i at $t + \Delta t$ for the intermediate nodes

$$u_i(t + \Delta t) = \frac{\theta_{slow}(t + \Delta t)\left(\mu_{i+1} - \mu_{i-1}\right)}{r_i(t + \Delta t)\left(r_{i+1}(t + \Delta t) - r_i(t + \Delta t)\right)}, \quad i = 1, \ldots, I - 1.$$

for the slow diffusion region, and

$$u_i(t + \Delta t) = \frac{\theta_{fast}(t + \Delta t)\left(\mu_{i+1} - \mu_{i-1}\right)}{r_i(t + \Delta t)\left(r_{i+1}(t + \Delta t) - r_i(t + \Delta t)\right)}, \quad i = I + 1, \ldots, N - 1.$$

for the superfast diffusion region.

9. From the boundary condition, the solution for the final spatial node is a constant

$$u_N(t + \Delta t) = 0.01.$$

10. Calculate the solution at the origin r_0,

$$u_0(t + \Delta t) = \frac{4\theta_{slow}(t + \Delta t)\mu_1}{(r_2(t + \Delta t))^2} - u_1(t + \Delta t),$$

as described in Section 3.

11. Calculate the updated solution at the interface,

$$u_I(t + \Delta t) = \frac{u_0(t + \Delta t)}{5}.$$

4 Results

This chapter contains the numerical results for the three diffusion cases

1. Slow with mass conservation,

2. Superfast with mass fraction conservation, and

3. Slow and superfast combined diffusion regimes.

In the first part we discuss the results of the slow diffusion using a moving mesh and conservation of mass in $2d$ radial coordinates, and the limitations on the stability of the scheme using different numerical methods to identify the solutions to the first and last nodes along the discretised r axis, depending on mesh discretisation.

4.1 Slow diffusion with mass conservation, where $m=1$

We shall firstly address the scenario where we have only slow diffusion, with mass conservation, as described in Section 3.1. Figure 8 shows the solution profile of $u(r,t)$ as function of spatial and temporal nodes, where $\Delta t = 0.001$, and for 32 spatial nodes at a separation of $\frac{1}{4\sqrt{5}}$.

When Δt is increased to 0.011 we see that the solution profile (Figure 9) appears to be unstable at the early spatial nodes, at early time. This can also be seen to be the case in Figure 9 at the final spatial nodes, however the profile smooths out at later time. Above $\Delta t = 0.011$ the method fails, due to tangling.
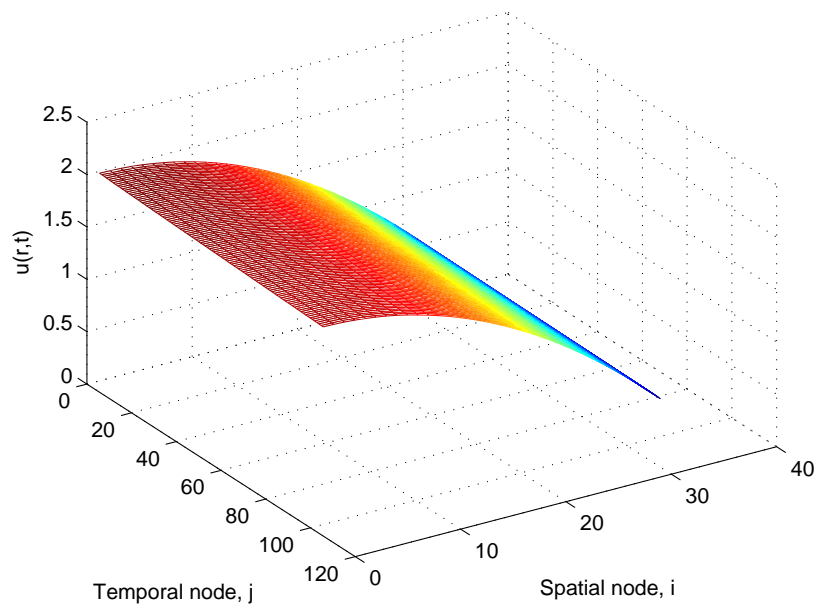
Figure 8: Numerical solution for u_i, where $\Delta r = \frac{1}{4\sqrt{5}}$ and $\Delta t = 0.001$

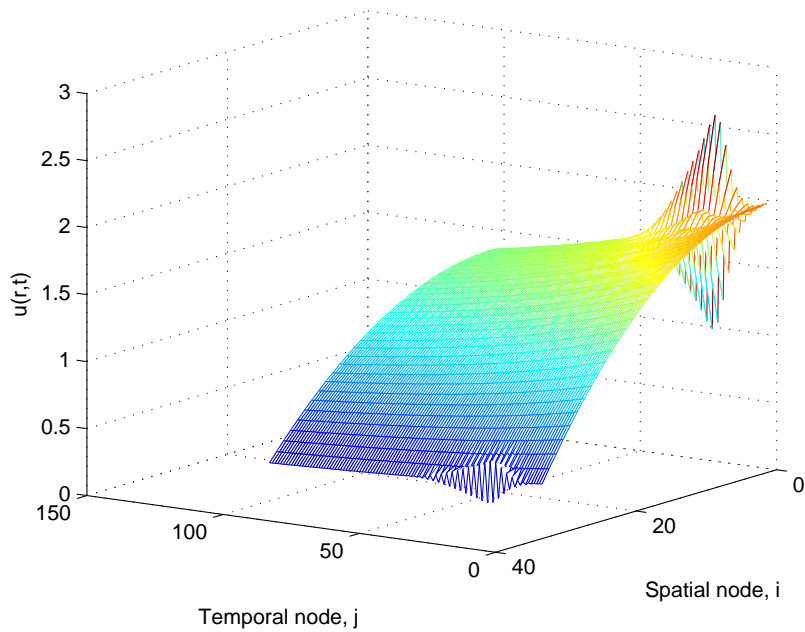

Figure 9: Numerical solution for u_i, where $\Delta r = \frac{1}{4\sqrt{5}}$ and $\Delta t = 0.011$

We can can apportion the instability to the choice of Δt. The scheme is only stable if there is a Courant-Friedrichs-Lewy (CFL) condition applied to the numerical scheme,

where, as previously mentioned, we have approximated the partial derivative $\frac{\partial u}{\partial r}$ using a central difference scheme

$$\left.\frac{\partial u}{\partial r}\right|_i \approx \frac{u_{i+1}^j - u_{i-1}^j}{r_{i+1}^j - r_{i-1}^j}$$

The CFL condition in this Lagrangian context is

$$|(v_{i+1} - v_i)\Delta t| < |r_{i+1} - r_i|. \tag{38}$$

For this slow, with constant mass diffusion scheme, this only applies where $\Delta t < 0.011$, i.e. intuitively, the distance moved ($|(v_{i+1} - v_i)\Delta t|$) via the calculated velocities using finite differences, must be less than that calculated by the difference in adjacent nodal positions for that time step. Figure 10 shows the velocities calculated for the stable scheme where $\Delta t = 0.001$.

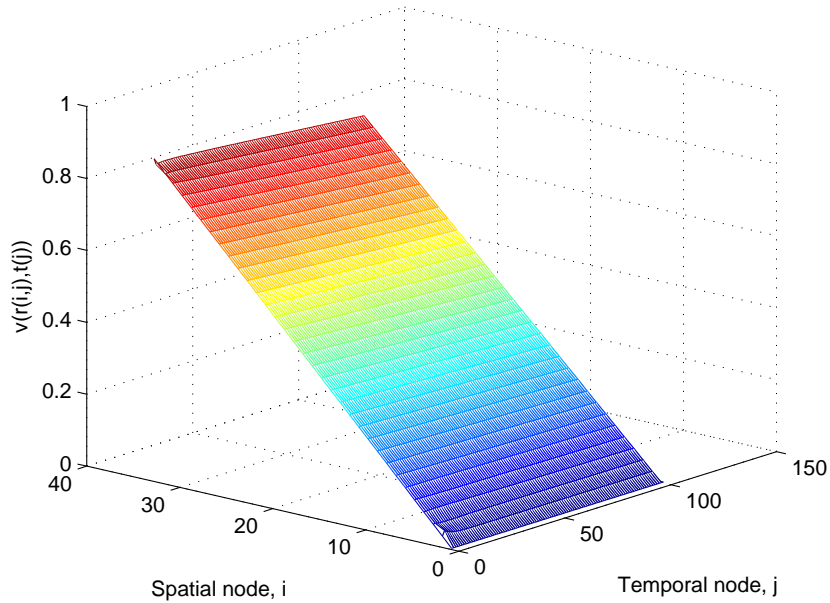

Figure 10: Numerical solution for v_i, where $\Delta r = \frac{1}{4\sqrt{5}}$ and $\Delta t = 0.001$

It can be seen from Figure 10 that the nodal velocities increase further away from the origin at $r_0 = 0$, as concentration / saturation of species decreases, and that the velocities, particularly those furthest from r_0, decrease slightly with time.

40

4.2 Superfast diffusion regime with constant mass fractions

In order to run a numerical test on the model we required an initial profile at t_0, with boundary conditions

$$u = 0.01 \quad \text{and} \quad urv + u^m r \frac{\partial u}{\partial r} = 0 \quad \text{at} \quad r(t) = r_N(t).$$

The parabola from the start of the superfast diffusion regime at t_0 is shown in Figure 11 and is given by equation (22).
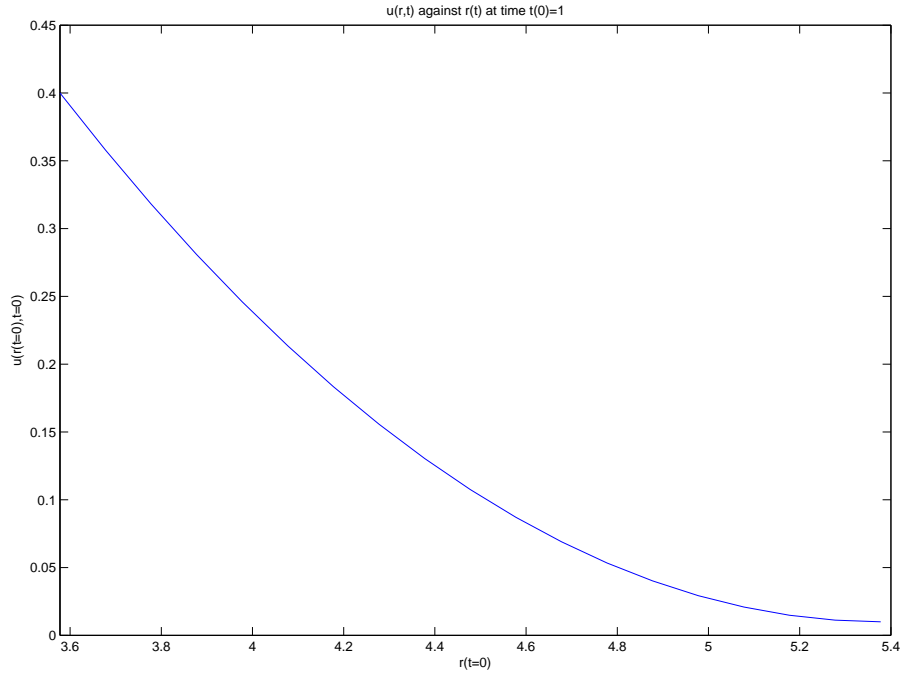

Figure 11: Initial profile for superfast diffusion regime, from r_0 and $t_0 = 1$. $\Delta r = \frac{1}{4\sqrt{5}}$.

Each spatial node, at a general time t, progresses with the velocity v_i. For a time step of 2×10^{-5}, and spatial step size $\Delta r = \frac{1}{4\sqrt{5}}$ (as was used for the slow diffusion with constant mass fractions), the method is stable. A $3D$ plot of the numerical solution to u_i is shown in Figure 12.
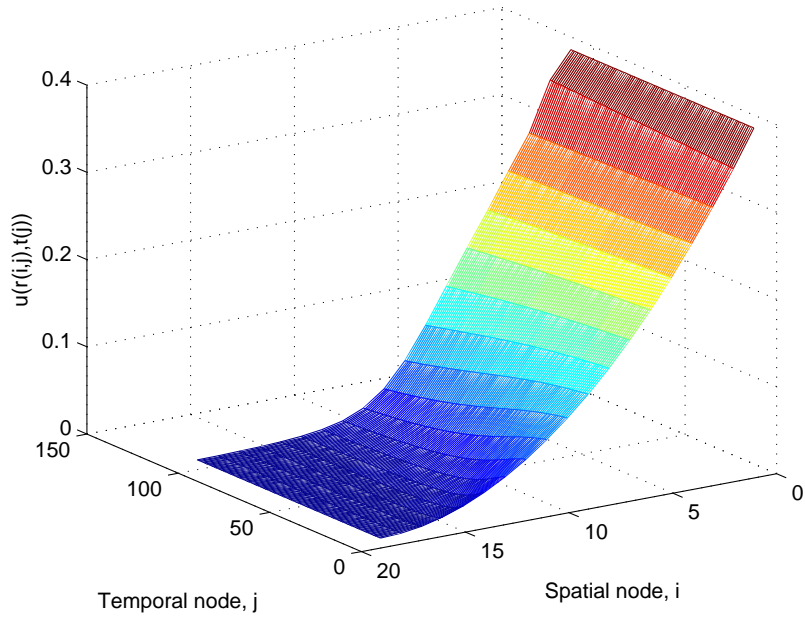
41

Figure 12: Numerical solution for u_i, where $\Delta t = 2 \times 10^{-5}$ and $\Delta r = \frac{1}{4\sqrt{5}}$.

Upon investigating Δt however, it is found that instability occurs above $\Delta t = 5 \times 10^{-5}$. This can be attributed to that fact that we are using an explicit methods to update the parameters within the superfast diffusion numerical model. The CFL condition is therefore violated above this limit of Δt.

Figure 13 shows the increase in nodal velocity (where the CFL condition is adhered to) for for a time step of $\Delta t = 2 \times 10^{-5}$. It can again be seen that over time, as was the case for slow diffusion, that although the nodal velocity increases with distance away from the origin, the velocity starts to decrease (Figure 14) at later times. It will eventually be zero at the point where the capillary bridge network breaks down, due to low u, and there is therefore, insufficient capillary bridge pressure to drive solvent migration.
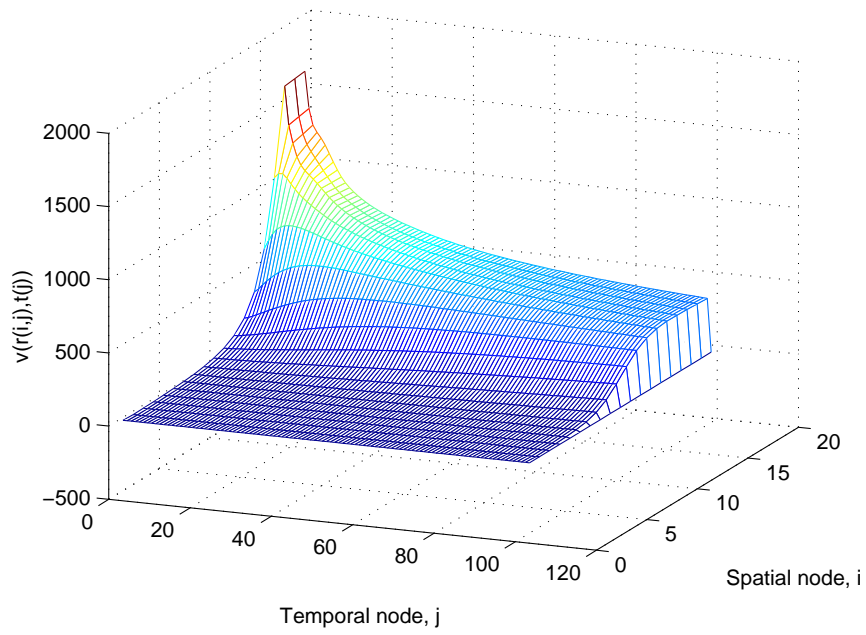
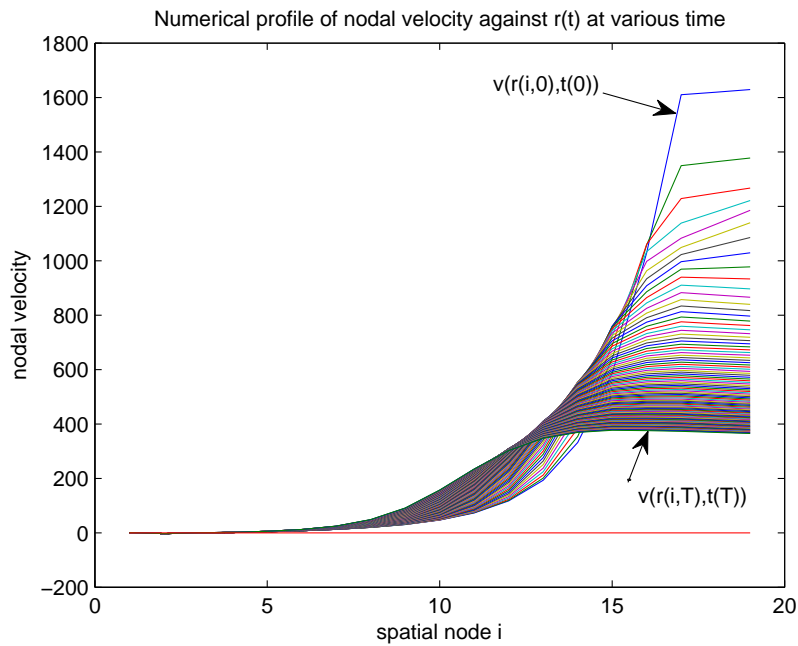Figure 13: Numerical solution for v_i, where $\Delta t = 2 \times 10^{-5}$ and $\Delta r = \frac{1}{4\sqrt{5}}$.

Figure 14: Numerical solution for velocity v_i against spatial node i for $t_0 = 1$ to $t(T)$, T=total number of time steps, $\Delta t = 2 \times 10^{-5}$ and $\Delta r = \frac{1}{4\sqrt{5}}$.

Figure 15 shows the increase in instability of nodal velocity as Δt increases towards
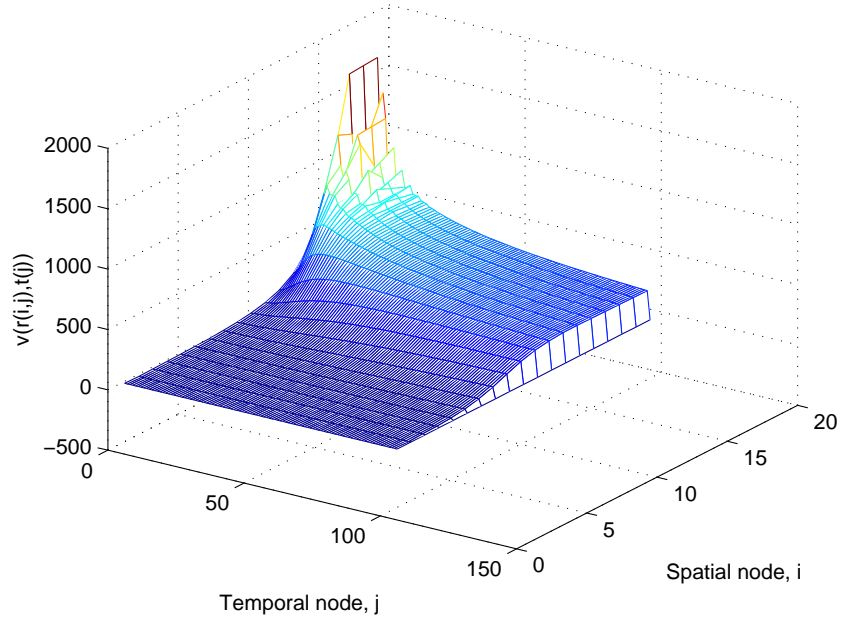
the limit of the CFL condition.

Figure 15: Numerical solution for v_i, where $\Delta t = 5 \times 10^{-5}$ and $\Delta r = \frac{1}{4\sqrt{5}}$.

In the superfast diffusion scheme, there is a more stringent requirement on Δt than in the slow regime. Above $\Delta t = 5 \times 10^{-5}$ the CFL condition is broken, and the numerical method fails.

4.3   Combined slow and fast diffusion regime

In this final section of the results we discuss the finite difference moving mesh method where we have joined the slow and superfast diffusion algorithms by calculating a velocity for the interface node, as described in the Section 3.6. We have considered that mass is no longer constant in both regimes, since it flows from the slow to the superfast region. However, the mass fractions between all adjacent nodes throughout the domain are forced to be constant.

The calculation of the velocity of the interface node $v_i(t)$ has proved successful in simply glueing the two different regimes together, however it is by no means smooth, as can be seen in the $3D$ plot of Figure 16 for a small time step $\Delta t = 2 \times 10^{-5}$, and the final plot of u_i against r_i in Figure 17. The velocity of the nodes progressing through the fast regime is seen to dramatically increase, particularly at early times, as seen in

44

Figure 18. The velocities of the nodes decrease with increasing time, and the velocity-space-time profile flattens out. This is in keeping with the experimental observations that as time progresses, the liquid furthest from the origin $r_0(t)$ will eventually stop, when there is no longer any driving pressure from liquid in the capillary bridges. This can be a long period of time, as described in reference [2].
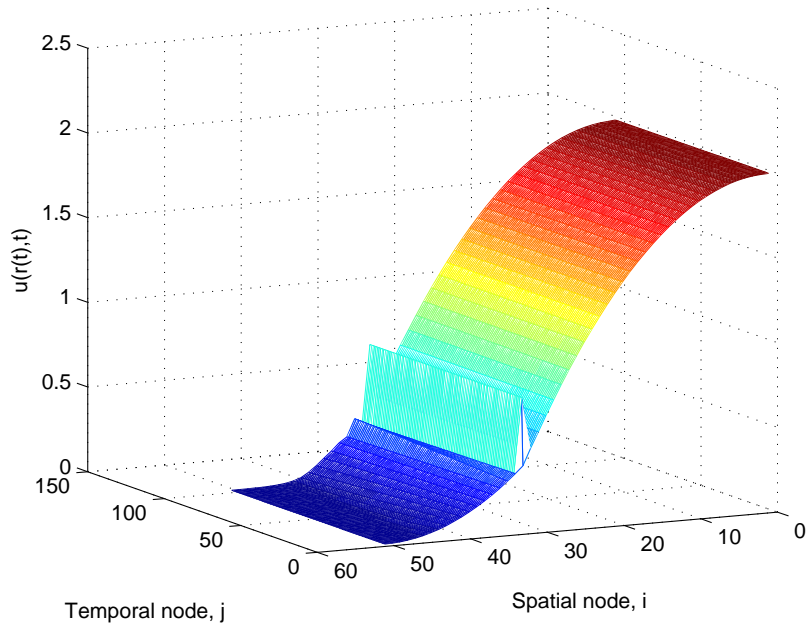

Figure 16: Numerical solution for u_i, in the combined slow-superfast regime, where $\Delta t = 2 \times 10^{-5}$ and $\Delta r = \frac{1}{4\sqrt{5}}$ at t_0.
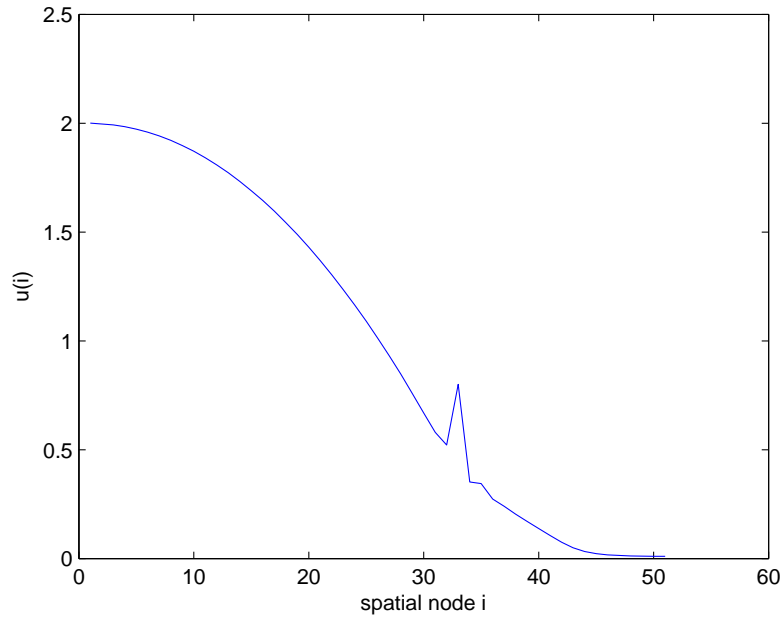
Figure 17: Numerical solution for u_i, in the combined slow-superfast regime, where $\Delta t = 2 \times 10^{-5}$ and $\Delta r = \frac{1}{4\sqrt{5}}$ at the final time.
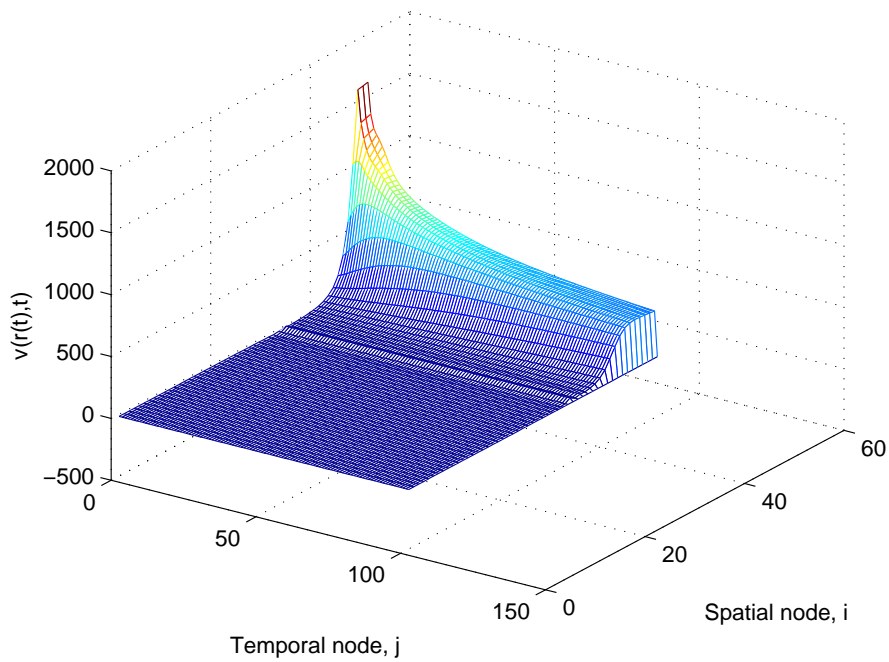

Figure 18: Numerical solution for v_i, where $\Delta t = 2 \times 10^{-5}$ and $\Delta r = \frac{1}{4\sqrt{5}}$ at t_0.

If the interface slope is approximated by a one sided finite difference approximation

on either side of the interface, i.e

$$\frac{\partial u}{\partial r}\bigg|_I \approx \frac{u_I - u_{I-1}}{r_I - r_{I-1}} \quad \text{on } \textit{slow} \text{ diffusion side of interface}$$

and

$$\frac{\partial u}{\partial r}\bigg|_I \approx \frac{u_{I+1} - u_I}{r_{I+1} - r_I} \quad \text{on } \textit{superfast} \text{ diffusion side of interface}$$

as opposed to the central difference method across the interface

$$\frac{\partial u}{\partial r}\bigg|_I \approx \frac{u_{I+1} - u_{I-1}}{r_{I+1} - r_{I-1}},$$

little improvement is seen in the smoothness of the profile. It may be necessary to change the resolution, i.e, decrease Δr, on either side of the boundary.

5 Discussion and Conclusions

In this section we discuss the implications and conclusions from the results.

This project has looked at the numerical modelling of both slow and superfast diffusion through a porous medium in a two dimensional radial domain. The method has considered only non volatile, non reacting species and explicit finite difference schemes to approximate partial derivatives $\frac{\partial u}{\partial r}$. The project has looked at superfast diffusion modelled by a moving mesh scheme based on constant mass fractions, where mass enters the superfast domain from the left hand boundary condition, where a self similar solution is used in the slow domain to determine the values at the interface.

The moving mesh finite difference method has proved successful in modelling the profile of concentration of the species against space and time, however with limitations on the time step, dependent on the CFL condition.

The method for modelling slow diffusion with constant mass over the domain has proved successful, providing that $\Delta t < 0.011$ for the specified $\Delta r = \frac{1}{4\sqrt{5}}$ at t_0. This avoids spatial nodes overtaking one another, thus ensuring that the CFL condition (equation (38)) is met. For slow diffusion with constant mass between nodes, we specified a boundary condition on the final node furthest from the origin $r_I(t)$,

$$u(r_I, t) = \frac{1}{5}u(r_0, t),$$

which, if the solvent was allowed to continue to migrate, would mark the start of the superfast diffusion regime, with a flux entering the boundary from the slow region. The interface marks a change in the value of m in equation (1) from $m = 1$ in the slow region to $m = -3/2$ in the superfast region. We used the conservation of mass to derive an expression at time t for the nodal velocities between the boundaries

$$v_i = -\left.\frac{\partial u}{\partial r}\right|_i \quad i = 1, \ldots, I-1,$$

which was approximated using using finite differences. The trapezoidal method was successfully used to calculate the solution $u_0(t)$.

The method for modelling superfast diffusion with constant mass fractions has a more

stringent Δt requirement than the simple case of slow diffusion with contant mass. For stability in this regime, it is required that $\Delta t < 5 \times 10^{-5}$. This limitation is to adhere to the CFL condition.

In this method the value of $u_I(t)$, at the left hand boundary of the domain, was calculated using the self-similar solution, equation (8). The velocity $v_I(t)$ was also derived from the self similar solution equation (13) . A central difference approximation was used in the calculation of the velocities of the nodes, to approximate $\frac{\partial u}{\partial r}$.

Additionally, both methods are given more stability when linear extrapolation is used to calculate the velocity of the final node in order to advance the mesh for the next time step.

Finally we presented a method for approximating an overall combined slow/superfast diffusion regime, where the value of m in the diffusion regime changed from $m = 1$ to $m = -3/2$ at the interface. The method hinged on the determination of the velocity at the interface node, which was calculated prior to the velocities of intermediate nodes in both of the slow and superfast regimes. As in the case of the slow diffusion in isolation, $u_0(t)$ was determined using the trapezoidal method. The join of slow and superfast diffusion profiles at the interface was not smooth, regardness of whether central or one-sided differences were used. It may be that the mesh size must be reduced/refined in the interface region in order to improve accuracy.

6 Recommendations for future work

Throughout the course of this study we have made a number of assumptions, one of the main ones being that it is possible to model a transition between the porous medium equation for the slow regime where $m = 1$, and for the superfast regime, where $m = -3/2$. This change between $m = -1$ and $m = -3/2$, is in reality likely to involve a gradual reduction of m as the saturation level of the solvent/concentration of the solvent decreases. From a modelling perspective, it may be more realistic to include a *number* of interfaces, say $i = I_1, I_2, \ldots, I_R$ for R changes in m. As in the algorithm for the combined diffusion in this study, it may be that a number of interface nodal velocities then need to be calculated, prior to the velocities of the nodes in the intermediate positions between the interfaces.

It has been seen throughout the results section, that the use of explicit finite difference method to approximate velocities $v_i(t)$ and solution values $u_I(t)$ has resulted in limitations on the value of the time steps Δt that can be used in the numerical method. It has been shown that a CFL condition must be adhered to, in order to ensure that "'node overtaking"' does not occur, at which point the method will fail. It is therefore suggested that an implicit method be used for the time stepping in order to avoid the "'trial and error"' method of determining the largest time step that can be used before node overtaking becomes an issue. Further details of implicit methods for moving boundaries can be found in reference [12]. This would also allow us to take a larger, more practical time step, to reduce the computational time that would be needed for very complex model problems, and avoiding the need to follow the Lagrangian type CFL condition. In order to smooth out the solution profile at the interface, and improve accuracy, it may be necessary to reduce/refine the mesh spacings Δr in the region around the interface. Indeed, a further development may be to investigate a moving mesh finite element method. This is a commonly used method, particularly for complex geometry systems, and further details can be found in [6], [10] and [13], where the latter reference includes finite element methods for homogeneous and inhomogenous solvents in porous materials.

In addition, practically there are a large number of physical systems in the environment that would include gradual evaporation of the solvent from the porous medium (likely

to involve a temperature and pressure dependence). A progression for this study could therefore include another term in the porous medium equation that would change the masses calculated between nodes with time. This could include evaporation rates at a particular temperature. Also possible is the addition of another source term, whether that be another species, or constant ingress of the solvent.

An additional progression would be to advance the moving mesh method from a 2 dimensional study to $3D$. Looking at the studies such as those in [2], a proposed model could be validated by a $3D$ fluorescence imaging techniques.

Bibliography

[1] Dullien, F. A. L.„ *Porous media. Fluid transport and pore structure*, second ed., Academic Press, San Diego, 1992.

[2] Lukyanov, A. V., Sushchikh, M. M., Baines, M. J. and Theofanous, T. G., *Superfast nonlinear diffusion: capillary transport in particulate porous media*, Phys. Rev. Lett.,**109**, 2012, 214501.

[3] Vazquez, J. L., *The porous medium equation - Mathematical theory*, Oxford Mathematical Monographs, Oxford University Press, Oxford, 2006.

[4] Rye, R. R., Yost, F. G. and O'Toole, E. J., *Capillary flow in irregular surface grooves*, Langmuir,**14**, 1998, 3937.

[5] Lee, T. E., Baines, M. J., Langdon, S. and Tindall, M. J., *A moving mesh approach for modelling avascular tumour growth.* Applied Numerical Mathematics, **72**, 2013, 99.

[6] Baines, M. J., Hubbard, M. E. and Jimack, P. K., *A moving mesh finite element algorithm for the adaptive solution of time dependent partial differential equations with moving boundaries*, Commun. Comput. Phys.,**10**, 2011, 509.

[7] Morton, K. W. and Mayers, D. F., *Numerical solution of partial differential equations*, second ed., Cambridge University Press, Cambridge, 2005.

[8] Logan, J. D., *An introduction to non-linear partial differential equations*, second ed., Wiley, New Jersey, 2008.

[9] Osman, K., *MSc Thesis: Numerical schemes for a non-linear diffusion problem*, University of Reading, 2005.

[10] Prince, J., *MSc Thesis: Fast diffusion through porous media*, University of Reading, 2011.

[11] Barenblatt, G. I., *Scaling*, Cambridge University Press, Cambridge, 2003.

[12] Baines, M. J. and Lee, T. E., *A large time-step implicit moving mesh scheme for moving boundary problems.* Num. Methods for Partial Differential Equations, **72**, 2013, 99.

[13] Pinder, G. F. and Gray, W. G., *Finite element simulation in surface and subsurface hydrology*, Academic Press, New York, 1977.